Limnol. Oceanogr., 57(4), 2012, 1182–1200

doi:10.4319/lo.2012.57.4.1182

Iron–light interactions differ in Southern Ocean phytoplankton

Robert F. Strzepek,[a,1,*] Keith A. Hunter,[a] Russell D. Frew,[a] Paul J. Harrison,[b] and Philip W. Boyd [c,d]

[a] Department of Chemistry, University of Otago, Dunedin, New Zealand
[b] Department of Earth and Ocean Sciences, University of British Columbia, Vancouver, Canada
[c] National Institute of Water and Atmospheric Research, Centre for Chemical and Physical Oceanography, Department of Chemistry, University of Otago, Dunedin, New Zealand
[d] National Institute of Water and Atmospheric Research, Greta Point, Wellington, New Zealand

Abstract

In laboratory experiments we examined the interplay of light and iron availability on the intracellular iron concentrations, specific growth rates, and photosynthetic physiology of Southern (S.) Ocean diatoms (*Eucampia antarctica* and *Proboscia inermis*) and the haptophyte *Phaeocystis antarctica*. Intracellular iron concentrations and iron : carbon (Fe : C) molar ratios increased with decreasing irradiance in temperate coastal (*Thalassiosira weissflogii*) and oceanic (*Thalassiosira oceanica*) diatoms, in support of the well-established antagonistic iron–light relationship. In contrast, S. Ocean species required lower cellular iron concentrations and Fe : C ratios than temperate diatoms to grow at comparable rates, and their iron requirements decreased or remained relatively constant with decreasing light. These results suggest that the current paradigm that low light increases algal cellular iron requirements (supplied through "biodilution") is not applicable to S. Ocean phytoplankton. Although iron use efficiencies decreased at sub-saturating light in all species, these reductions were due primarily to lower growth rates, but not higher intracellular Fe : C ratios, in S. Ocean species. We propose that S. Ocean species have overcome the antagonistic iron–light relationship by increasing the size, rather than the number, of photosynthetic units under low irradiances, resulting in an acclimation strategy that does not increase their cellular iron requirements.

Over the last 15 yr, numerous experiments have provided compelling evidence that iron availability both limits phytoplankton growth and influences community structure in ~ 30% of the world ocean (Boyd et al. 2007). The Southern (S.) Ocean has received the greatest attention regarding the biogeochemical implications of iron availability because it is the largest iron-limited region, has a major influence on the global carbon cycle (via both ocean circulation and biogeochemistry), and is reported to be the most sensitive biogeochemical province to future climate change (Sarmiento et al. 1998, 2010). Although iron limitation plays a major role in maintaining high-nitrate, low-chlorophyll (HNLC) conditions across much of the S. Ocean, other environmental factors also contribute to this HNLC condition (Boyd 2002). Most significantly, light limitation of phytoplankton productivity can be pronounced because of deep seasonal mixed layers caused by vigorous wind mixing, in combination with low incident irradiances due to extensive cloud and seasonal ice cover (Mitchell et al. 1991; Nelson and Smith 1991).

Modeling studies predict that multiple environmental properties of S. Ocean waters will be altered concurrently by climate change: surface waters will become warmer and fresher, with increased vertical stratification, shallower mixed-layer depths, reduced sea-ice volume, and higher oceanic carbon dioxide (CO_2) concentrations (Sarmiento et al. 2004; Boyd et al. 2007). Changes in the physical and chemical environment will consequently affect light, macronutrient and trace metal supply, pH, and CO_2 concentrations—the key determinants regulating phytoplankton carbon fixation, biomass, and export. Such climate change–mediated alteration of surface-water properties in the S. Ocean will not occur independently; therefore, the synergistic and antagonistic effects of altered water properties need to be considered when assessing future phytoplanktonic responses (Boyd et al. 2010).

There is ongoing debate as to whether low iron and light supply co-regulate phytoplankton growth in the S. Ocean (Sunda and Huntsman 1997; Galbraith et al. 2010), and how to define such co-regulation or co-limitation (Saito et al. 2008). Central to this debate is the concept that light may modulate the cellular iron requirements of phytoplankton, thereby affecting both the onset and degree of iron limitation in natural systems, and consequently the magnitude of carbon fixation. Thus, a key unknown in future predictions of biological CO_2 removal from the atmosphere in response to changes in iron availability is the codependence of phytoplankton physiology on light and iron (Sarmiento et al. 2010), and how different formulations of this codependence affect the response of ecosystems to changes in iron supply. Although iron limitation is explicitly included in numerous biogeochemical–ecosystem models, its implementation varies. For example, a common feature of these models is to treat the effects of low iron and low light as antagonistic, such that phytoplankton iron requirements increase under low light, thus increasing their susceptibility to iron limitation (Aumont and Bopp 2006; Mongin et al. 2007; J. P. Dunne unpubl.).

The antagonistic iron–light relationship that is used to parameterize such models is derived from both theoretical

* Corresponding author: robert.strzepek@anu.edu.au

[1] Present address: Research School of Earth Sciences, The Australian National University, Canberra, Australia

calculations of the iron costs to drive algal physiology at low vs. high light levels (Raven 1990) and subsequent experimental evidence using temperate phytoplankton in a suite of detailed lab culture experiments (Sunda and Huntsman 1997). Indirect support for this paradigm has come from several laboratory studies that reported enhanced cellular iron concentrations in low-light-acclimated phytoplankton (Strzepek and Price 2000; Strzepek and Harrison 2004; Finkel et al. 2006). However, the extent to which the trends reported for the interplay of iron and light on temperate phytoplankton species, from both coastal and offshore waters (Sunda and Huntsman 1997), apply to the S. Ocean is not known.

Iron addition to natural S. Ocean phytoplankton assemblages has been reported to increase maximum photosynthetic rates (P^B_{max}), quantum efficiencies (approximated from the initial slope of the photosynthesis–irradiance relationship, α^B), and the chlorophyll-to-carbon ratio (θ), suggesting that iron-replete cells can utilize the light they intercept to assimilate CO_2 more effectively (Hopkinson et al. 2007; Hiscock et al. 2008). The physiological basis that underpins this iron–light concept is the high and essential requirement for iron in the electron transport pathways that accomplish photosynthesis (Raven 1990; Strzepek and Harrison 2004). As cells acclimate to low light, cellular iron requirements may increase depending on which photoacclimatory strategy they employ (Fig. 1).

Given the relevance of iron and light interactions to the S. Ocean, several shipboard (Boyd et al. 1999; Moore et al. 2007) and lab studies have investigated particular aspects of iron–light interactions using the resident phytoplankton, but have provided no clear consensus. The field studies in subantarctic waters suggest that both iron and light can limit phytoplankton productivity seasonally, where iron is limiting in late austral spring and summer, but iron and irradiance may be co-limiting in early spring (Boyd et al. 1999; Boyd et al. 2001). During the Crozet natural iron bloom and export experiment, Moore et al. (2007) found that only one of the five shipboard iron–light perturbation experiments showed some evidence of antagonistic iron–light co-limitation. Lab culture studies, each using different S. Ocean species and a range of experimental conditions, have also provided evidence both for (Timmermans et al. 2001) and against (Hoffman et al. 2008) an antagonistic iron–light relationship in S. Ocean diatoms.

The principal goal of the present study was to determine how iron and light limitation affect the physiology and iron content of a range of S. Ocean species. In this study, we report the first intracellular iron concentrations and iron-to-carbon ratios for iron-limited and iron-replete S. Ocean phytoplankton grown over a range of light intensities. Moreover, we sought to determine if phytoplankton grown under low light and low iron supply are simultaneously co-limited by these resources, and thus build upon the comprehensive assessment of iron–light interactions in temperate phytoplankton species, such as those used in the seminal iron–light study of Sunda and Huntsman (1997).

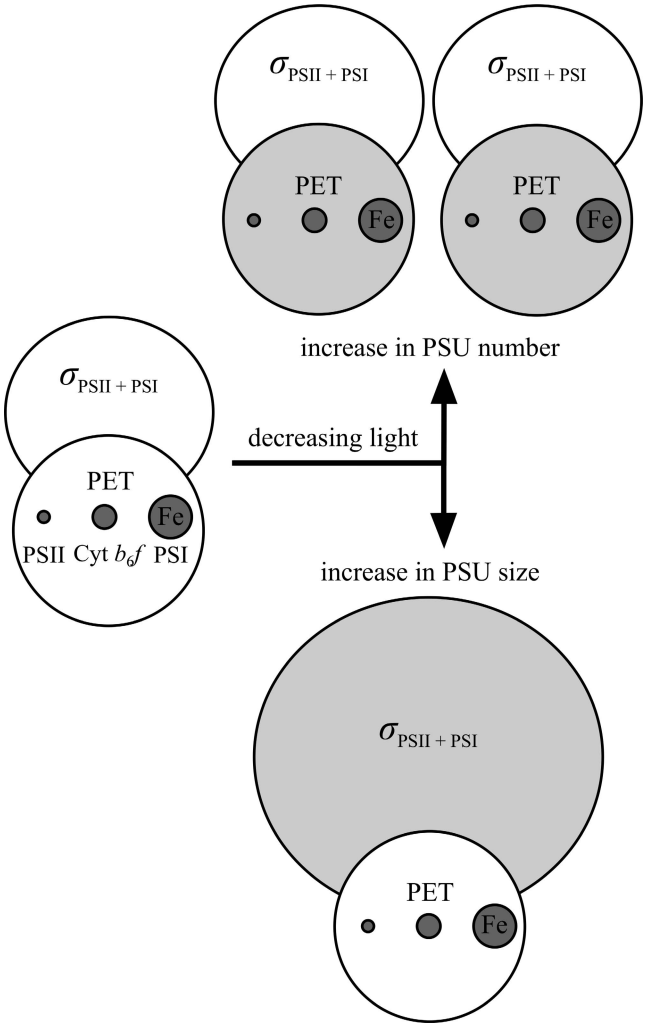

Fig. 1. Schematic of how photoacclimation may alter the iron requirements for photosynthesis by marine phytoplankton. Acclimation to low light may involve increases in photosynthetic unit (PSU) number (top) or size (bottom). Changes due to acclimation are shown in light gray. An increase in PSU number will increase the cellular concentrations of the iron-rich protein complexes that accomplish photosynthetic electron transport (PET). PET is catalyzed by photosystem II (PSII), the cytochrome b_6f complex (Cyt b_6f) and photosystem I (PSI). The relative iron (Fe) content of the complexes is depicted by the size of the dark circles (2–3 atoms of Fe per PSII, 5 atoms of Fe per Cyt b_6f, and 12 atoms of Fe per PSI). An increase in PSU size is accomplished through higher amounts of light-harvesting pigments and their arrangement, and is reflected in the functional absorption cross section for light absorption ($\sigma_{PSII} + \sigma_{PSI}$). This acclimation strategy does not increase cellular iron requirements. Importantly, this simplified schematic assumes that the photosystems and their associated light-harvesting antennae change in concert. In reality, photosystem abundance, σ_{PSII}, and σ_{PSI} may change independently (Suggett et al. 2007). Moreover, these two photoacclimation strategies are not mutually exclusive (Falkowski and La Roche 1991).

Methods

Study organisms—Growth irradiance manipulation experiments were performed on four S. Ocean isolates

collected south of the Polar Frontal Zone in December 2001 (the centric diatoms *Proboscia inermis* and *Eucampia antarctica*, and *Phaeocystis antarctica* [clone AA1]) and in December 2004 (*Phaeocystis antarctica* [clone SX9]). Stable monocultures were established by July 2002 (June 2005 for *P. antarctica* clone SX9). These phytoplankton species have been observed to bloom upon purposeful or natural iron fertilization of S. Ocean waters (Strzepek et al. 2011). Experiments on *P. antarctica* (clone AA1) were completed in 2005; experiments on the other S. Ocean isolates were completed in 2008. All results reported for *P. antarctica* (clone AA1) are for solitary cells; *P. antarctica* (clone SX9) retained the ability to form colonies at the time of sampling. The growth rates of S. Ocean isolates in the experimental media attained steady state within the pre-acclimation period of two transfers (14–16 generations) and remained stable over the 6-yr period of the study (*see* fig. 1 of Strzepek et al. 2011). In order to cross-reference our findings for S. Ocean phytoplankton isolates, we also examined two well-studied temperate diatoms of the genus *Thalassiosira*: *Thalassiosira oceanica* (clone 1003), an oceanic isolate from the Sargasso Sea, and the coastal isolate *Thalassiosira weissflogii* (clone Actin, Long Island Sound, New York). Both were obtained from the Provasoli-Guillard Center for Culture of Marine Phytoplankton (West Boothbay Harbor, Maine) and maintained under axenic conditions.

Medium preparation—All phytoplankton cultures were grown in the artificial seawater medium Aquil enriched with 10 μmol L^{-1} phosphate, 100 μmol L^{-1} silicate, 300 μmol L^{-1} nitrate, and filter-sterilized (0.2 μm Gelman Acrodisc PF) trace metal and vitamin solutions as described in Strzepek et al. (2011).

The basal Aquil medium contained 1.8 $\pm$ 0.1 nmol L^{-1} iron (Fe) contamination (n = 6), measured using electrochemical techniques, which was included in the calculation of total iron (Strzepek et al. 2011). For S. Ocean isolates, iron-replete medium contained a total of 4.4 nmol L^{-1} Fe and 10 μmol L^{-1} ethylenediaminetetraacetic acid (EDTA). Due to the photo-lability of Fe-EDTA chelates, inorganic iron concentrations ([Fe′]) ranged from 107–1170 pmol L^{-1} from 10–570 μmol quanta m^{-2} s^{-1}. [Fe′] were calculated for Fe-EDTA media following Sunda and Huntsman (2003) at the mean incubation temperature (3°C) and at pH 8.3—the mean pH of the initial media (8.17 $\pm$ 0.04) and late-exponential-phase cultures (8.4 $\pm$ 0.02). Overall conditional steady-state dissociation constants for Fe-EDTA chelates ranged from 2.67 $\times$ 10^{-6} at 570 μmol quanta m^{-2} s^{-1} and 2.45 $\times$ 10^{-7} at 10 μmol quanta m^{-2} s^{-1}. Therefore, the $[Fe_{total}]$: [Fe′] ratio ranged from 3.7 at high light to 40.8 at low light in Aquil media containing 4.4 nmol L^{-1} Fe and 10 μmol L^{-1} EDTA. The overall conditional dissociation constant was calculated as the sum of the conditional stability constant in the dark (2.01 $\times$ 10^{-7}) and the conditional photo-dissociation constant (K_{hv}; 2.17 $\times$ 10^{-6} multiplied by I_{hv}, the light intensity relative to 500 μmol quanta m^{-2} s^{-1}) of EDTA at 3°C. K_{hv} at 3°C was estimated from values at 10°C and 20°C (Sunda and Huntsman 2003), assuming that K_{hv} is a linear function of temperature.

In order to induce iron stress in the S. Ocean isolates, iron was added complexed with the terrestrial siderophore desferrioxamine B mesylate (DFB; Sigma-Aldrich). Iron-limiting media were designed to reduce growth rates at growth-saturating irradiance by ~ 50%. Therefore, the Fe : DFB ratios (nmol L^{-1} : nmol L^{-1}) in iron-limiting Aquil media differed between isolates: *Phaeocystis* strains—Fe : DFB 3.8 : 400; *Proboscia inermis*—Fe : DFB 3.8 : 200; *Eucampia antarctica*—Fe : DFB 3.8 : 40 (hereafter referred to as Fe : DFB 4 : 400, 4 : 200, and 4 : 40, respectively). [Fe′] in FeDFB media were calculated by the equation [Fe′] = [FeDFB]/([L′] $\times$ $K_{Fe'L}^{cond}$) ($K_{Fe'L}^{cond}$ = $10^{11.8}$ measured in Aquil at pH 8; Maldonado et al. 2005).

T. oceanica and *T. weissflogii* were grown in high-iron Aquil medium containing 58.3 nmol L^{-1} Fe and 10 μmol L^{-1} EDTA ([Fe′] = 1290–2670 pmol L^{-1}), and low-iron medium containing 4.4 nmol L^{-1} Fe and 10 μmol L^{-1} EDTA ([Fe′] = 96–201 pmol L^{-1}). [Fe′] were calculated for pH 8.3 and 18°C as described above. Overall conditional steady-state dissociation constants for Fe-EDTA chelates at 18°C ranged from 4.60 $\times$ 10^{-7} at 280 μmol quanta m^{-2} s^{-1} to 2.20 $\times$ 10^{-7} at 20 μmol quanta m^{-2} s^{-1}. Note that the iron-replete Aquil medium for S. Ocean isolates and the iron-limiting medium for temperate isolates had identical total iron and EDTA concentrations (4.4 nmol L^{-1} Fe, 10 μmol L^{-1} EDTA), but [Fe′] were higher at 3°C compared to 18°C (~ 1.3–2-fold over a comparable irradiance range) due to the effect of lower temperature increasing the photo-dissociation constant for Fe-EDTA chelates (Sunda and Huntsman 2003).

Light manipulation experiments—S. Ocean experimental cultures were grown in triplicate, maintained in exponential phase by dilution, and allowed to acclimate to growth conditions for at least two transfers (14–16 cell divisions) before data collection from steady-state-acclimated cultures. *P. antarctica* (clone AA1) was grown at 3°C under continuous light at eight photon flux densities (PFDs; 3, 10, 20, 30, 60, 100, 400, and 570 μmol quanta m^{-2} s^{-1}) obtained using cool-white fluorescent bulbs (13W Standard, Sylvania). PFDs were measured with a calibrated 4π quantum meter (model QSL-2101, Biospherical Instruments). The other three S. Ocean isolates were grown at 3°C under continuous light at five PFDs (10, 20, 30, 60, and 100 μmol quanta m^{-2} s^{-1}). Experimental cultures of *T. oceanica* and *T. weissflogii* were grown at five continuous PFDs (20, 40, 70, 100, and 280 μmol quanta m^{-2} s^{-1}) at 18°C. Growth rates of acclimated cells were determined from in vivo chlorophyll *a* (Chl *a*) fluorescence using a Turner Designs model 10-AU fluorometer. Specific growth rates (d^{-1}) were calculated from least-squares regressions of ln in vivo fluorescence vs. time during the exponential growth phase.

Growth vs. irradiance curves were determined by plotting specific growth rate (μ), against growth irradiance (E_{gr}) and fitting the equation of MacIntyre et al. (2002) to the data:

$$\mu = \mu_{max}\left(1 - \exp\left[-A_{gr}E_{gr}/\mu_{max}\right]\right) \quad (1)$$

where μ_{max} is the light-saturated growth rate, and A_{gr} is the initial slope of the growth-irradiance curve. The growth saturation parameter (K_E) is calculated as

$$K_E = \mu_{max}/A_{gr} \quad (2)$$

Cellular iron, carbon, and chlorophyll a *concentrations*—To measure intracellular iron and cellular carbon concentrations, cultures were incubated with ^{14}C-bicarbonate (specific activity $\sim$ 28 kBq; PerkinElmer) and $^{55}FeCl_3$ (specific activity 920–2015 MBq L^{-1}; PerkinElmer) following Strzepek et al. (2011). The specific activity of the ^{55}Fe radiotracer in Aquil media ranged from 2.23×10^9 to 9.52×10^9 MBq mol^{-1} Fe, and accounted for 25–65% of the total iron concentration. Phytoplankton completed at least eight cell divisions before harvesting to ensure uniform labeling. Cellular chlorophyll *a* (Chl *a*) concentrations were determined for *P. antarctica* (clone AA1) by in vitro fluorometry on a Turner Designs model 10-AU fluorometer calibrated with spectrophotometrically measured spinach Chl *a* standards (Sigma-Aldrich). Samples were extracted in 90% acetone in the dark for $<$ 24 h at -20°C prior to analysis.

Cell size (fL $cell^{-1}$ [fL = femtoliter = 10^{-15} L]) and cell density (cells mL^{-1}) were determined by Coulter Counter® (Model ZM) and microscopy (Palmer Mahoney chamber). *P. antarctica* and the temperate *Thalassiosira* diatom species were counted and sized by both microscopy and Coulter Counter; no significant difference between methods was observed. Coulter Counter measurements were performed on freshly harvested cultures. Microscopy counts were conducted at the time of harvest or within 1 week of preservation with 0.4% glutaraldehyde. Cell dimensions were always measured in freshly harvested cultures using a calibrated ocular micrometer. Cell volumes and surface areas were calculated assuming the following geometric approximations: *P. antarctica*—sphere; *E. antarctica*—cube; *P. inermis* and *Thalassiosira* spp.—cylinder.

Fast repetition rate and pulse amplitude modulated (PAM) fluorometry—Fast repetition rate (FRR) fluorometry was used to calculate the maximum photochemical efficiency of photosystem II (PSII), $F_v : F_m$ (where $F_v = F_m - F_o$) for the S. Ocean isolates. The FRR technique fully reduces the primary electron acceptor, Q_A, and allows a simultaneous single closure of all PSII reaction centers (single turnover [ST]). A Chelsea Instruments FASTtracka FRR fluorometer was programmed to acquire ST saturations of PSII from 100 flashlets of 1.1 μs applied at 2.8-μs intervals. Each acquisition consisted of 10 such sequences applied at 1-s intervals. The minimum (F_o) and maximum (F_m) fluorescence and the effective absorption cross section (σ_{PSII}) of PSII reaction centers were determined by fitting the biophysical model of Kolber et al. (1998) to the mean of 10–20 acquisitions using the v6 software provided by Sam Laney (Oregon State University). Fluorescence data were corrected for both instrument nonlinearities (Laney and Letelier 2008) and sample blanks (0.2-μm-filtered culture; Cullen and Davis 2003). The units for σ_{PSII} are nm^2 $quanta^{-1}$ ($100\ nm^2 = 1\ Å^2$) and the values are specific to the excitation wavelength emitted by the bank of blue light-emitting diodes of the instrument with peak output at 478 nm. σ_{PSII} values are therefore referred to as σ_{PSII} (478). The ST protocol described here resulted in PSII saturation (F_m) after 50–70 flashlets.

All fluorescence measurements were made once algal samples had been dark-acclimated for 30–45 min at 4°C (S. Ocean isolates) or 18°C (temperate isolates). FRR measurements were made directly in the 28-mL polycarbonate culture tubes, which were placed in the light chamber of the FRR. Measurements of F_o, F_m, and σ_{PSII} from samples measured in a homemade quartz cuvette placed in the light chamber or samples poured directly into the dark chamber of the FRR were not significantly different from those made in the culture tubes ($p > 0.05$; data not shown).

$F_v : F_m$ was also measured with a Phyto-PAM fluorometer (Walz) equipped with a Phyto-ED emitter–detector unit programmed to acquire multiple turnover (MT) saturations of PSII using a 200–300-ms saturation flash applied at 30-s intervals. The inter-pulse interval was determined from the minimum time required for fluorescence to relax to pre-saturation levels. Before FRR analysis, a 4-mL aliquot was transferred from each tube to a cylindrical quartz cuvette for Phyto-PAM measurements. The mean $F_v : F_m$ value from four excitation wavelengths (470, 520, 645, and 665 nm) was calculated for each saturation flash, and a minimum of 10 saturation flashes was averaged for each sample. A Water-S stirring device (Walz) was used to keep samples suspended, and was shut off 10 s before applying each saturation flash to minimize signal noise. Only the Phyto-PAM was used to measure $F_v : F_m$ of the temperate isolates.

Data analysis—Sample means and standard errors were calculated using Microsoft Excel software (version 2011 for Macintosh). Data were examined for normality and equal variance prior to analysis of variance and Tukey–Kramer means comparison tests to determine treatment effects (Prism 5 for Mac, GraphPad Software). Significant results are reported at the 95% confidence level ($p < 0.05$). Nonlinear regression analyses were performed using Prism 5.

Results

Iron, light availability, and phytoplankton growth rates—The growth rates of all isolates were reduced by iron limitation at all growth irradiances, but the effect of iron limitation on growth rate was less pronounced in light-limited cultures for five of the six isolates (Fig. 2). Iron-limited growth rates are expressed both in absolute terms (μ_{-Fe}) and relative to iron-replete growth rate (μ_{+Fe}) at the same growth irradiance ($\mu_{-Fe} : \mu_{+Fe}$; calculated using discrete rather than model growth rate data). In all isolates except *T. oceanica*, growth rates of iron-replete and iron-limited cultures converged with decreasing irradiance and, consequently, $\mu_{-Fe} : \mu_{+Fe}$ increased. In contrast to the other

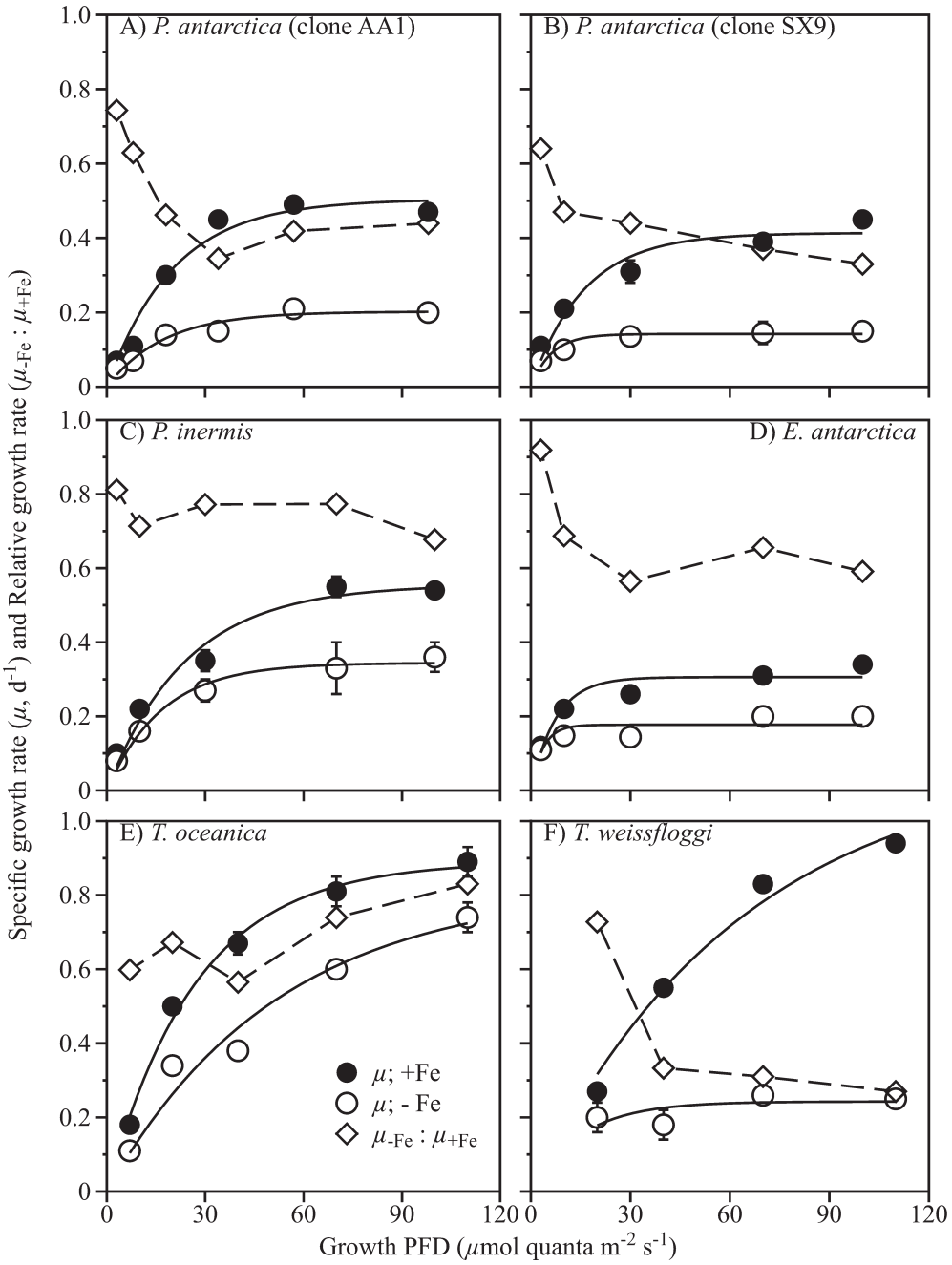

Fig. 2. Steady-state specific growth rates of (A–D) four S. Ocean and (E, F) two temperate phytoplankton isolates over a range of irradiances (photon flux density, PFD). (A) *Phaeocystis antarctica* (clone AA1); (B) *Phaeocystis antarctica* (clone SX9); (C) *Proboscia inermis*; (D) *Eucampia antarctica*; (E) *Thalassiosira oceanica*; and (F) *Thalassiosira weissflogii*. Relative iron limitation of growth rate ($\mu_{-Fe}:\mu_{+Fe}$) equals the rate observed under iron limitation divided by the maximum iron-replete rate at the same growth irradiance. The solid lines represent the best fit to Eq. 1. Error bars represent standard error and are smaller than the symbol when not visible (n = 3–16). Some of the data (E, F) for the temperate diatoms are from Strzepek and Harrison (2004). A subset of these data for the S. Ocean isolates were published in Boyd et al. (2010).

isolates, $\mu_{-Fe}:\mu_{+Fe}$ progressively decreased with declining irradiance for *T. oceanica* (Fig. 2E).

We also measured the growth of *P. antarctica* (clone AA1) cultures at two higher growth irradiances: 400 and 570 μmol quanta m^{-2} s^{-1}. Growth rates declined significantly ($p < 0.05$) in both iron-replete and iron-limited cultures at these higher irradiances, resulting in a distinct growth rate maximum between 60–100 μmol quanta

m^{-2} s^{-1} (Fig. 3D; Table 1). Repeated attempts to grow iron-limited cultures of *P. antarctica* (clone AA1) at 570 μmol quanta m^{-2} s^{-1} were unsuccessful.

Specific growth rates of all species were reduced at decreased irradiances and were generally well described by the exponential equation of MacIntyre et al. (2002) ($R^2 > 89$; Table 2). The two exceptions were iron-limited cultures of *E. antarctica* ($R^2 = 0.58$) and *T. weissflogii* ($R^2 = 0.33$), where growth rates differed little between the highest and lowest irradiances.

Parameters derived from the growth–irradiance relationship (Eqs. 1, 2) revealed that K_E (the light level where growth rate begins to saturate) was not significantly different among the isolates but for three exceptions (Table 2): (1) K_E of *E. antarctica* was significantly lower than the other isolates under both iron-replete and iron-limited conditions, suggesting that growth of this species saturates at very low irradiances (< 7.5 μmol quanta m^{-2} s^{-1}); (2) K_E of iron-replete *T. weissflogii* cultures was

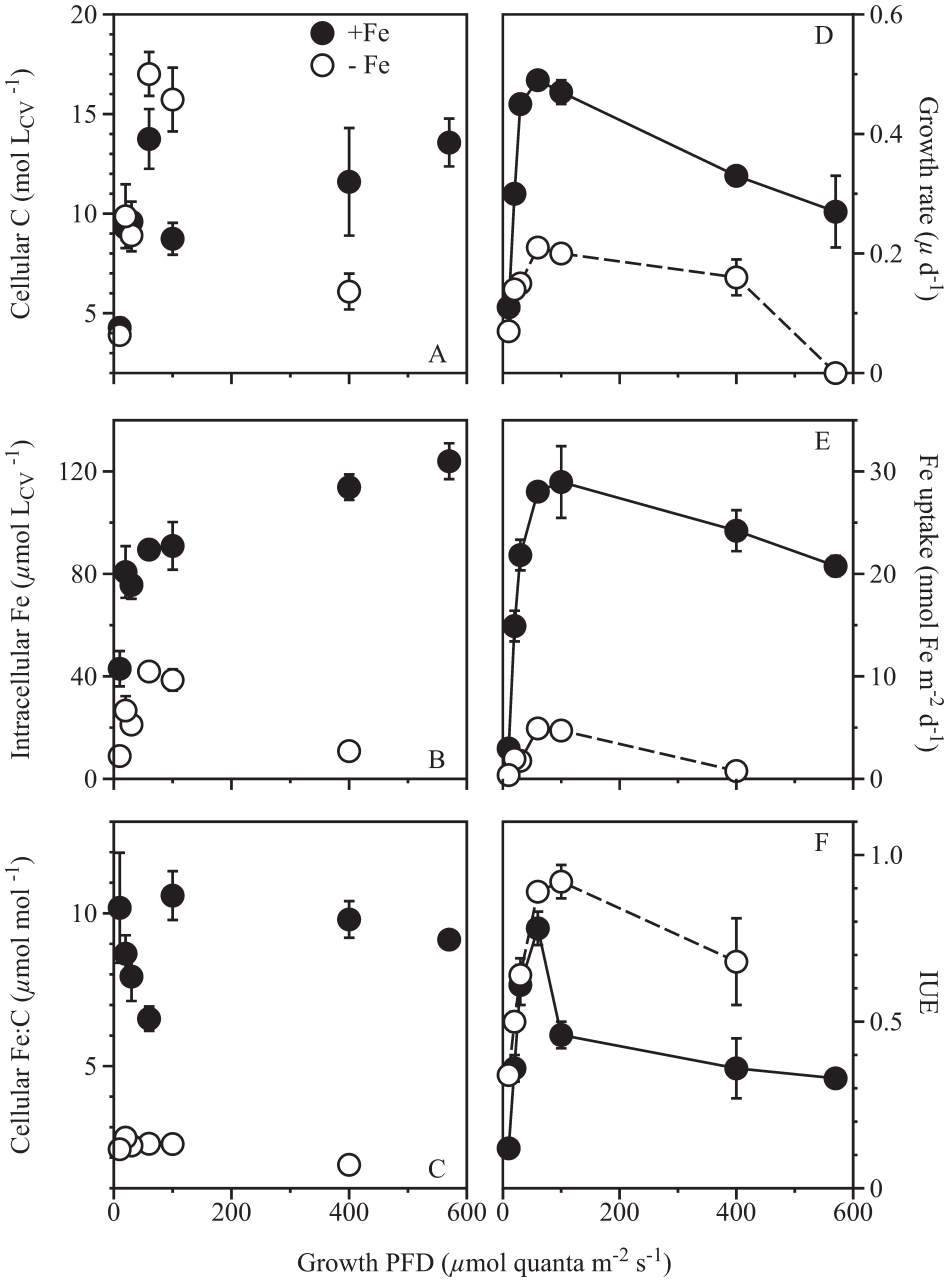

Fig. 3. Relationships between elemental and physiological properties of *P. antarctica* (clone AA1) and growth irradiance (photon flux density [PFD]). (A) Cell volume–normalized cellular carbon concentrations. (B) Cell volume–normalized intracellular iron concentrations. (C) Cellular Fe : C ratios. (D) Specific growth rate (μ). (E) Steady-state cell surface area–normalized iron uptake rate. (F) Iron use efficiency (IUE; units: $\times 10^5$ mol C mol^{-1} Fe d^{-1}). Error bars represent standard error and are smaller than the symbol when not visible (n = 3–16).

Table 1. Specific growth rates (μ) and cell volume–normalized intracellular iron (Fe) and cellular carbon (C) concentrations of phytoplankton as a function of iron availability and growth irradiance (PFD, μmol quanta m^{-2} s^{-1}). Values within parentheses are standard error (n = 3–12). "ng" indicates "no growth." Steady-state iron uptake rates are normalized to cell surface area (nmol Fe m^{-2} d^{-1}). Units for iron use efficiency (IUE) are $\times 10^5$ mol C mol^{-1} Fe d^{-1}. The intracellular iron concentrations of iron-replete cultures of *T. oceanica* and *T. weissflogii* have been reported previously (Strzepek and Harrison 2004).

Species	Iron treatment	Growth PFD	[Fe′]* (pmol L^{-1})	Growth rate (d^{-1})	Cell volume (CV) (fL $cell^{-1}$)	Fe concentration (μmol L_{CV}^{-1})	C concentration (mol L_{CV}^{-1})	Fe : C (μmol mol^{-1})	Steady-state Fe uptake	IUE
P. antarctica	Iron-replete	570	1170	0.27(0.06)	15.6(0.4)	124(7)	13.6(1.3)	9.1(0.1)	20.8(1.0)	0.33(0.01)
(clone AA1)	(4.4 nmol L^{-1}	400	845	0.33(0.01)	18.6(0.4)	114(5)	11.6(2.7)	9.8(0.6)	24.2(2.0)	0.36(0.09)
	Fe; 10 μmol L^{-1}	100	277	0.47(0.02)	27.1(3.9)	90.9(9.3)	8.7(0.8)	10.6(0.8)	29.0(3.5)	0.46(0.04)
	EDTA)	60	202	0.49(0.01)	24.0(0.7)	89.5(1.0)	13.7(1.5)	6.5(0.4)	28.0(0.8)	0.78(0.05)
		30	145	0.45(0.01)	20.5(1.0)	75.7(5.4)	9.6(1.0)	7.9(0.8)	21.8(1.5)	0.61(0.06)
		20	126	0.30(0.01)	20.2(0.9)	80.7(10.1)	9.3(0.6)	8.7(0.6)	14.9(1.5)	0.36(0.04)
		10	107	0.11(0.00)	18.5(1.6)	43.0(6.9)	4.3(0.5)	10.2(1.8)	3.0(0.6)	0.12(0.02)
	Iron-limited	570	0.02	ng						
	(Fe : DFB	400	0.02	0.16(0.03)	17.7(1.2)	10.8(2.8)	6.1(0.9)	1.8(0.1)	0.8(0.0)	0.68(0.13)
	4 : 400)	100	0.02	0.20(0.01)	15.0(0.2)	38.6(4.2)	15.7(1.6)	2.5(0.0)	4.7(0.7)	0.92(0.05)
		60	0.02	0.21(0.01)	14.6(0.5)	41.9(3.2)	17.0(1.1)	2.5(0.0)	4.9(0.4)	0.89(0.01)
		30	0.02	0.15(0.00)	15.5(1.0)	21.2(1.5)	8.9(0.8)	2.4(0.1)	1.8(0.1)	0.64(0.05)
		20	0.02	0.14(0.01)	15.5(0.2)	26.7(5.6)	9.9(1.6)	2.7(0.2)	1.9(0.4)	0.50(0.03
		10	0.02	0.07(0.01)	17.1(0.8)	8.9(0.7)	3.9(0.2)	2.3(0.2)	0.4(0.1)	0.34(0.03)
E. antarctica	Iron-replete	100	277	0.33(0.01)	15,200(750)	9.5(0.9)	5.3(0.7)	1.8(0.1)	11.1(0.9)	1.89(0.17)
	(4.4 nmol L^{-1}	30	145	0.26(0.02)	19,300(400)	5.3(0.6)	3.0(0.5)	1.8(0.0)	4.5(0.6)	1.42(0.14)
	Fe; 10 μmol L^{-1}	10	107	0.21(0.02)	23,300(330)	1.2(0.1)	1.0(0.2)	1.1(0.02)	1.0(0.1)	1.92(0.07)
	EDTA)									
	Iron-limited	100	0.17	0.20(0.03)	24,000(1500)	1.4(0.1)	1.5(0.1)	0.93(0.06)	1.3(0.1)	2.42(0.12)
	(Fe : DFB 4 : 40)	30	0.17	0.14(0.02)	11,100(400)	2.2(0.1)	2.3(0.1)	0.94(0.03)	0.9(0.1)	1.49(0.07)
		10	0.17	0.14(0.00)	11,900(500)	2.6(0.2)	2.0(0.1)	1.3(0.0)	1.0(0.1)	1.13(0.01)
P. inermis	Iron-replete	100	277	0.51(0.02)	43,800(4400)	5.0(0.3)	1.1(0.1)	4.5(0.2)	7.95(0.74)	1.11(0.11)
	(4.4 nmol L^{-1}	30	145	0.44(0.01)	50,400(2900)	1.9(0.1)	1.5(0.1)	0.9(0.02)	3.01(0.14)	5.17(0.79)
	Fe; 10 μmol L^{-1}	10	107	0.22(0.01)	57,000(2100)	0.94(0.15)	1.3(0.4)	0.7(0.00)	0.86(0.17)	2.99(0.13)
	EDTA)									
	Iron-limited	100	0.03	0.31(0.02)	53,500(2300)	0.21(0.04)	0.55(0.07)	0.37(0.06)	0.28(0.07)	8.16(0.40)
	(Fe : DFB	30	0.03	0.30(0.01)	51,600(3700)	0.20(0.03)	0.50(0.04)	0.40(0.07)	0.26(0.04)	7.67(2.00)
	4 : 200)	10	0.03	0.14(0.01)	55,900(3500)	0.32(0.03)	1.19(0.24)	0.29(0.07)	0.19(0.02)	4.91(1.02)
T. oceanica	Iron-replete	280	2670	1.03(0.05)	71.3(2.8)	382(15)	17.0(0.3)	22.5(0.3)	14.8(0.63)	0.44(0.01)
	(58 nmol L^{-1}	110	1780	0.89(0.04)	69.2(2.4)	486(76)	19.1(0.8)	25.4(1.5)	16.3(0.92)	0.32(0.01)
	Fe; 10 μmol L^{-1}	70	1560	0.81(0.04)	77.7(5.8)	529(26)	22.3(2.7)	23.7(1.5)	15.6(0.88)	0.35(0.02)
	EDTA)	40	1400	0.67(0.03)	59.6(0.5)	450(2)	16.4(1.0)	27.4(0.5)	8.34(0.29)	0.19(0.01)
		20	1290	0.50(0.01)	77.2(3.7)	420(6)	17.5(1.8)	24.0(1.3)	7.78(2.00)	0.20(0.02)
	Iron-limited	280	201	0.78(0.05)	47.6(1.0)	39.0(3.5)	16.2(2.3)	2.2(0.1)	1.10(0.18)	3.15(0.45)
	(4.4 nmol L^{-1}	110	132	0.74(0.04)	47.7(3.7)	71.1(1.1)	19.6(1.9)	3.6(0.1)	1.67(0.07)	2.20(0.07)
	Fe; 10 μmol L^{-1}	70	116	0.60(0.01)	66.2(0.6)	76.8(0.6)	22.0(3.3)	3.5(0.2)	1.66(0.37)	1.72(0.43)
	EDTA)	40	104	0.38(0.01)	55.8(2.1)	66.3(0.9)	23.0(1.6)	2.8(0.1)	0.84(0.05)	1.33(0.09)
		20	96	0.34(0.00)	69.9(2.2)	78.8(5.8)	17.1(1.2)	4.6(0.1)	1.25(0.14)	0.90(0.11)
T. weissflogii	Iron-replete	280	2670	1.04(0.04)	1160(3)	518(40)	15.0(0.1)	33.9(1.3)	49.2(4.5)	0.31(0.01)
	(58 nmol L^{-1}	110	1780	0.94(0.01)	1250(58)	463(30)	8.9(0.4)	52.2(0.3)	40.8(2.5)	0.18(0.00)
	Fe; 10 μmol L^{-1}	70	1560	0.83(0.01)	946(15)	442(52)	8.2(0.2)	54.1(0.4)	31.8(3.7)	0.15(0.00)
	EDTA)	40	1400	0.55(0.01)	809(38)	620(12)	12.5(0.7)	49.5(0.5)	27.6(0.4)	0.11(0.00)
		20	1290	0.27(0.00)	650(13)	942(16)	14.8(0.9)	71.9(1.9)	19.4(2.3)	0.04(0.00)

Table 1. Continued.

Species	Iron treatment	Growth PFD	[Fe′]* (pmol L^{-1})	Growth rate (d^{-1})	Cell volume (CV) (fL $cell^{-1}$)	Fe concentration (μmol L_{CV}^{-1})	C concentration (mol L_{CV}^{-1})	Fe : C (μmol mol^{-1})	Steady-state Fe uptake	IUE
	Iron-limited	280	201	0.27(0.01)	346(22)	53.5(12.0)	15.8(4.9)	3.4(0.3)	0.87(0.30)	0.80(0.04)
	(4.4 nmol L^{-1}	110	132	0.25(0.02)	428(26)	54.7(1.1)	8.7(2.7)	6.3(0.2)	0.90(0.07)	0.40(0.03)
	Fe; 10 μmol L^{-1}	70	116	0.26(0.02)	665(39)	55.5(2.8)	8.1(1.3)	6.9(0.1)	1.05(0.12)	0.37(0.04)
	EDTA)	40	104	0.18(0.04)	499(69)	65.3(1.5)	9.3(1.0)	7.1(0.1)	0.81(0.19)	0.26(0.07)
		20	96	0.20(0.04)	402(45)	63.4(9.6)	6.1(0.9)	10.4(0.1)	0.81(0.25)	0.19(0.05)

* [Fe′] > 700 pmol L^{-1} exceed the empirically observed threshold for precipitation of iron hydroxides (Sunda and Huntsman 1995) and are therefore overestimates.

significantly higher than the other iron-replete isolates; and (3) K_E of iron-limited *T. oceanica* cultures was significantly higher than the other iron-limited isolates. The response of *P. antarctica* (clone AA1) to iron limitation differed from the other five isolates with respect to initial slope of the growth-irradiance curve, A_{gr}, which decreased 2-fold under iron limitation (Table 2).

Taxonomic and environmental influences on cellular iron and carbon concentration—Cell volumes: The effects of iron and light availability on the cell volumes and the elemental composition of the isolates are summarized in Table 1. Growth rates for cultures harvested for elemental analyses are also presented, and differ slightly from the compiled data presented in Fig. 2, of which they are a subset. For *P. antarctica* (clone AA1), maximum cell volumes were observed in iron-replete cells grown between 60–100 μmol quanta m^{-2} s^{-1}. Iron-limited cells of *P. antarctica* were generally smaller than iron-replete cells, but this difference was significant only between 20–100 μmol quanta m^{-2} s^{-1} ($p < 0.05$). In contrast, cell volumes of *E. antarctica* and *P. inermis* did not change systematically with changes in iron or light supply (Table 1; $p > 0.05$).

Iron-limited cells of the *Thalassiosira* isolates were significantly smaller than iron-replete cells ($p < 0.05$; Table 1), particularly in *T. weissflogii* where iron limitation reduced cell volumes ~ 2-fold. Light limitation also reduced the cell volume of iron-replete cells of *T. weissflogii* by 1.7-fold. This effect of light on cell volumes was only observed in iron-replete cells of *T. weissflogii*.

Taxonomic trends in intracellular iron concentrations: We observed distinct taxonomic differences in cell volume-normalized intracellular iron concentrations, with a clear trend of decreasing intracellular iron concentration with increasing cell size. Under comparable culturing conditions (i.e., 4.4 nmol L^{-1} Fe and 10 μmol L^{-1} EDTA; 100–110 μmol quanta m^{-2} s^{-1}), intracellular iron concentrations ranged 18-fold: from 90.0 ± 9.3 μmol Fe per liter cell volume (L_{CV}^{-1}) for the smallest isolate, *P. antarctica* (clone AA1), to 5.0 ± 0.3 μmol Fe L_{CV}^{-1} for the large diatom *P. inermis*. Cellular carbon concentrations also decreased with cell size, ranging 17-fold among the isolates: from 19.6 ± 1.9 mol C L_{CV}^{-1} for *T. oceanica* to 1.1 ± 0.1 mol C L_{CV}^{-1} for *P. inermis*.

Intracellular iron concentrations and Fe : C ratios of *P. antarctica*: In exponentially growing cultures under steady-state conditions, iron uptake rates (V_{ss}; units: nmol Fe m^{-2} d^{-1}) can be calculated as the product of specific growth rate (μ) and cell surface area–normalized intracellular iron concentration:

$$V_{ss} = \mu \times \text{intracellular Fe} \quad (3)$$

Similarly, iron use efficiency (IUE)—the rate of carbon assimilation per unit of intracellular iron—was calculated by dividing μ by the intracellular Fe : C ratio (units: × 10^5 mol C mol^{-1} Fe d^{-1}):

$$\text{IUE} = \mu/\text{intracellular Fe : C} \quad (4)$$

By combining information on steady-state growth rates and elemental composition, we observed that, like steady-

Table 2. Growth rate parameters of phytoplankton isolates derived as a function of growth irradiance using data presented in Fig. 2. Values within parentheses are standard error (n = 3–12). Iron-limited values that are not significantly different from iron-replete values are denoted with an asterisk ($p < 0.05$).

Species	μ_{max}		A_{gr}		K_E		R^2	
	+Fe	−Fe	+Fe	−Fe	+Fe	−Fe	+Fe	−Fe
Phaeocystis antarctica (clone AA1)	0.50(0.03)	0.20(0.01)	0.025(0.003)	0.012(0.002)	20.2	17.4	0.97	0.94
Phaeocystis antarctica (clone SX9)	0.41(0.03)	0.14(0.01)	0.026(0.006)	0.023(0.005)*	16.0	6.2	0.93	0.89
Proboscia inermis	0.56(0.04)	0.34(0.02)	0.023(0.004)	0.021(0.003)*	24.2	16.8	0.97	0.98
Eucampia antarctica	0.31(0.02)	0.18(0.02)	0.041(0.010)	0.050(0.021)*	7.5	3.6	0.89	0.58
Thalassiosira oceanica	0.89(0.03)	0.82(0.12)*	0.033(0.022)	0.016(0.003)*	27.1	52.0	0.99	0.96
Thalassiosira weissflogii	1.17(0.15)	0.24(0.03)	0.018(0.002)	0.016(0.007)*	63.6	15.1	0.98	0.33

state growth rates, the cell surface area–normalized iron uptake rates (Fig. 3E), and IUEs (Fig. 3F) of *P. antarctica* (clone AA1) decreased both below and above an optimal irradiance range in both iron-replete and iron-limited cultures. In iron-replete cultures, both cell volume–normalized intracellular iron (Fig. 3B) and cellular carbon (Fig. 3A) concentrations decreased at irradiances below this growth optimum, but as intracellular iron concentrations decreased less than for carbon, a distinct "dip" in cellular Fe : C ratios was evident around the optimal growth irradiance (Fig. 3C). At supraoptimal irradiances, steady-state iron uptake rates decreased to a lesser extent than growth rates, resulting in an increase in intracellular iron concentration (Fig. 3B). In iron-limited cultures,

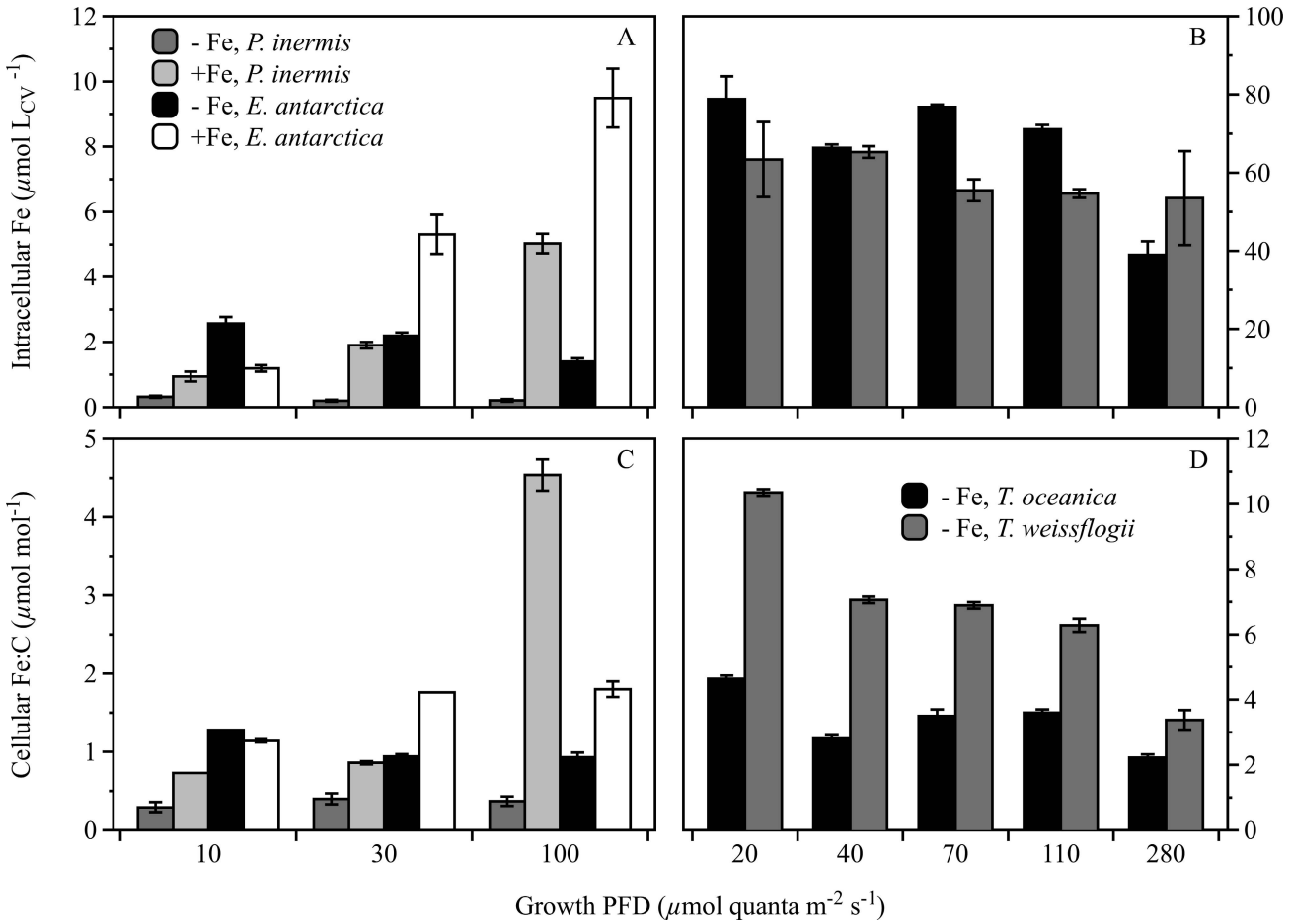

Fig. 4. Relationships between (A, B) cell volume–normalized intracellular iron concentrations, and (C, D) cellular Fe : C molar ratio and growth irradiance (photon flux density, PFD) for the (A, C) S. Ocean diatoms *E. antarctica* and *P. inermis* and (B, D) *T. weissflogii* and *T. oceanica*. Iron-replete S. Ocean isolates and iron-limited temperate isolates were grown at the same iron concentration (4.4 nmol L^{-1} Fe, 10 μmol L^{-1} EDTA) but [Fe′] were 1.3–2.1-fold greater at 3°C compared to 18°C over a comparable PFD range. Error bars represent standard error and are smaller than the symbol when not visible (n = 3–6). Note the different scales of the Intracellular Fe and Cellular Fe : C axes for (A, C) S. Ocean and (B, D) temperate diatom isolates.

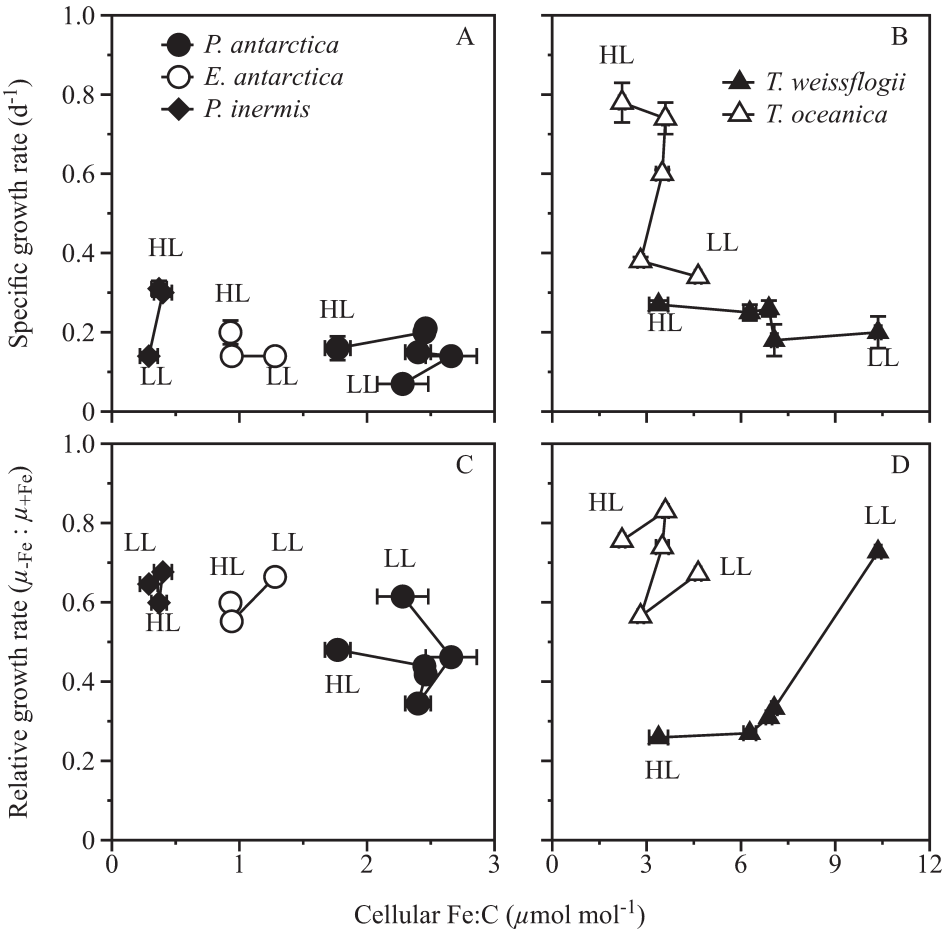

Fig. 5. (A, B) Specific growth rates (μ) and (C, D) relative growth rate growth rate ($\mu_{-\mathrm{Fe}} : \mu_{+\mathrm{Fe}}$) as functions of the cellular Fe : C ratio for iron-limited phytoplankton cultures grown over a range of photon flux densities (PFDs). For each phytoplankton species, lines connect growth irradiance treatments, with the highest and lowest growth irradiances indicated by "HL" and "LL," respectively. Error bars represent standard error and are smaller than the symbol when not visible (n = 3–6). Note the different scales of the Cellular Fe : C axes for (A, C) S. Ocean and (B, D) temperate phytoplankton isolates.

decreases in intracellular iron and cellular carbon concentrations both above and below the optimal growth irradiance were closely coupled, resulting in a nearly constant cellular Fe : C ratio over the full irradiance range.

Intracellular iron concentrations and Fe : C ratios of diatoms: In iron-replete S. Ocean diatoms, intracellular iron concentrations (Fig. 4A) were reduced with decreasing growth irradiance. With a 2.5-fold decrease in [Fe′] between 100 and 10 μmol quanta m^{-2} s^{-1}, steady-state iron uptake rates declined by 11-fold in *E. antarctica* and 9-fold in *P. inermis* (Table 1). As specific growth rates decreased less than iron uptake rates with decreasing irradiance, intracellular iron concentrations diminished 7.9-fold in *E. antarctica* and 5.3-fold in *P. inermis* (Fig. 4A). Cellular Fe : C ratios also decreased as light levels were reduced: 1.6-fold for *E. antarctica* and 6.4-fold for *P. inermis* (Fig. 4C).

In contrast, in iron-replete cultures of *T. oceanica*, reductions in both specific growth rate (2-fold) and iron uptake rates (1.9-fold) were closely coupled to decreases in [Fe′] (1.7-fold) as irradiance was lowered, resulting in relatively constant intracellular iron concentrations and cellular Fe : C ratios (Table 1). In iron-replete cultures of *T. weissflogii*, intracellular iron concentrations and cellular Fe : C ratio rose with decreasing irradiance (Table 1).

In iron-limited S. Ocean diatoms, small increases in intracellular iron concentrations with decreasing irradiance were observed. At a constant [Fe′] (as the Fe-DFB complex is not photo-reactive), both the specific growth and iron uptake rates of *E. antarctica* declined ~ 1.3-fold with reduced irradiance (Table 1), and the 1.9-fold increase in intracellular iron concentration (Fig. 4A) was mainly due to 2-fold smaller cell volumes at low light (Table 1). As cellular carbon content also increased at low light (1.3-fold), cellular Fe : C ratios remained relatively constant with changes in irradiance (Fig. 4C). In iron-limited *P. inermis* cultures, intracellular iron content was remarkably low, and increased 1.5-fold with reduced irradiance (Fig. 4A). As we observed for *E. antarctica*, the cellular Fe : C ratios of *P. inermis* were not significantly different among the light treatments ($p > 0.05$; Fig. 4C).

We observed much larger changes in the cellular Fe : C ratios of iron-limited *Thalassiosira* isolates with changes in

light intensity. Cellular Fe : C increased 2.1-fold in *T. oceanica* and 3-fold in *T. weissflogii* as irradiance was lowered (Fig. 4D). Changes in the Fe : C ratio of *T. oceanica* were driven principally by increasing intracellular iron concentrations with decreasing light (Fig. 4B), whereas in *T. weissflogii*, a 2.6-fold reduction in cellular carbon content was the main cause for the 3-fold higher Fe : C ratios at low light.

Taxonomic differences in the cellular iron required to support growth: Specific growth rates (μ) of iron-limited cultures were plotted as a function of their cellular Fe : C ratios under different light conditions (Fig. 5). We also examined how the relative growth rates ($\mu_{-Fe} : \mu_{+Fe}$, where μ_{+Fe} is the iron-replete growth rate at the same irradiance) varied with cellular Fe : C. Figure 5 illustrates two important findings. We observed distinct interspecific differences in the cellular Fe : C ratio required to support a given growth rate: S. Ocean diatoms required markedly lower (by as much as 20-fold) cellular Fe : C ratios to maintain specific growth rates (Fig. 5A) comparable to *T. weissflogii* (Fig. 5B,D). Among the S. Ocean isolates, cellular iron requirements decreased with cell size: *P. inermis* < *E. antarctica* < *P. antarctica*. These diatoms also required 3–6-fold lower cellular Fe : C than *T. oceanica* to attain comparable relative growth rates ($\mu_{-Fe} : \mu_{+Fe} \sim 0.6$–$0.7$) (Fig. 5C,D). However, absolute specific growth rates of *T. oceanica* were nevertheless ~ 2-fold higher at low light and ~ 4-fold higher at high light than the S. Ocean isolates (Fig. 5A,B).

We also observed species-specific changes in cellular iron requirements with changes in growth irradiance. For *T. weissflogii*, decreasing irradiance resulted in a 3-fold higher cellular Fe : C (Fig. 5B,D). This increase in Fe : C enabled *T. weissflogii* to attain higher $\mu_{-Fe} : \mu_{+Fe}$ at low light. Cellular Fe : C ratios also increased to lesser degree in *T. oceanica*, but the effect on $\mu_{-Fe} : \mu_{+Fe}$ was less pronounced than in *T. weissflogii* (Fig. 5B,D). For *P. antarctica*, the relationship between specific growth rate and cellular Fe : C was more complex, with Fe : C decreasing at the upper and lower bounds of the irradiance range (Fig. 5A,C). In contrast, the S. Ocean diatoms maintained relatively constant specific growth rates, relative growth rates, and cellular Fe : C (Fig. 5A,C).

The ability of S. Ocean diatoms to simultaneously maintain high rates of growth and low cellular Fe : C was reflected in their IUEs (Table 1). At ~ 100 μmol quanta m^{-2} s^{-1}, IUEs ranged 20–26-fold (high and low light, respectively) among the isolates and were greatest for the S. Ocean isolates and *T. oceanica*. IUEs of *P. antarctica* were markedly lower, falling between the values for oceanic diatoms and *T. weissflogii*. IUEs were reduced by about 50% in all species with decreasing light. In the S. Ocean isolates, reductions in IUEs were due primarily to lower growth rates, but not higher cellular Fe : C molar ratios, with decreasing light. In the temperate isolates, reduced IUEs were due to both decreases in growth rates and increases in cellular Fe : C ratios with declining irradiance.

Iron–light interactions and photophysiology—Phaeocystis antarctica cultures: $F_v : F_m$ declined linearly with increasing irradiance in both iron-replete and iron-limited cultures (Fig. 6A), and were consistently lower in iron-limited cultures compared to iron-replete cultures.

We observed large changes in σ_{PSII} of *P. antarctica* (clone AA1) in response to both light and iron availability (Fig. 6B). σ_{PSII} decreased 4.6-fold (3.3-fold when the highest light treatment is excluded) in iron-replete cultures and 2.7-fold in iron-limited cultures with increasing growth irradiance. On average, σ_{PSII} was 1.7-fold larger in iron-limited compared to iron-replete cultures.

Cellular Chl *a* increased in both iron-replete and iron-limited cultures with decreasing growth irradiance (Fig. 6C). Iron-limited cultures generally had lower cellular Chl *a* than iron-replete cultures, but this difference was modulated by growth irradiance. Iron-limited cultures grown at 400 μmol quanta m^{-2} s^{-1} were exceptionally chlorotic, containing ~ 7-fold lower Chl *a* than iron-replete cultures. At intermediate irradiances (20–100 μmol quanta m^{-2} s^{-1}), cellular Chl *a* concentrations were 2.4-fold lower in iron-limited cultures compared to iron-replete cultures and at 10 μmol quanta m^{-2} s^{-1}, cellular Chl *a* concentrations of iron-replete and iron-limited cultures were not statistically different ($p < 0.05$). While the fluorescence yield per unit of Chl *a* (F : Chl *a*) was relatively constant with growth irradiance in iron-replete cultures, it increased by ~ 7-fold in iron-limited cultures at growth irradiances ≥ 30 μmol quanta m^{-2} s^{-1} (Fig. 6D). This high F : Chl *a* in high-light, iron-limited cells is indicative of uncoupling of PSII antennae complexes from the reaction centers under iron limitation, with a greater proportion of absorbed light energy being re-emitted as fluorescence (Vassiliev et al. 1995).

Diatom cultures: $F_v : F_m$ decreased (Fig. 7A,B) and σ_{PSII} increased (Fig. 7C,D) under iron limitation in S. Ocean diatoms. σ_{PSII} was 1.7- and 1.4-fold larger in iron-limited relative to iron-replete cultures of *E. antarctica* and *P. inermis*, respectively. Among S. Ocean isolates, σ_{PSII} increased and maximum $F_v : F_m$ decreased significantly ($p < 0.05$) with increasing cell size, such that σ_{PSII} was largest in the large diatom *P. inermis* and the smallest in *P. antarctica*. Conversely, the maximum observed $F_v : F_m$ was lowest in *P. inermis* and highest in *P. antarctica*.

Phyto-PAM measurements of $F_v : F_m$ ($F_v : F_m$ (MT)) in S. Ocean isolates were 1.4–1.7-fold higher than FRR results, with the exception of iron-limited cultures of *P. inermis*, where the difference was 2.7-fold (data not shown). Maximum $F_v : F_m$ (MT) values were higher in the temperate diatoms compared to the S. Ocean isolates. In *T. weissflogii*, $F_v : F_m$ (MT) decreased with increasing irradiance in iron-replete cultures (0.74 ± 0.02 to 0.64 ± 0.01) and did not change significantly with changes in growth irradiance in iron-limited cultures (0.40 ± 0.01 to 0.38 ± 0.01). In *T. oceanica*, $F_v : F_m$ (MT) decreased with increasing irradiance in both iron-replete and iron-limited cultures: 0.71 ± 0.02 to 0.42 ± 0.02, and 0.66 ± 0.01 to 0.31 ± 0.03, respectively (data not shown).

Discussion

There is ongoing debate as to whether low iron and light supply co-regulate phytoplankton growth in the S. Ocean

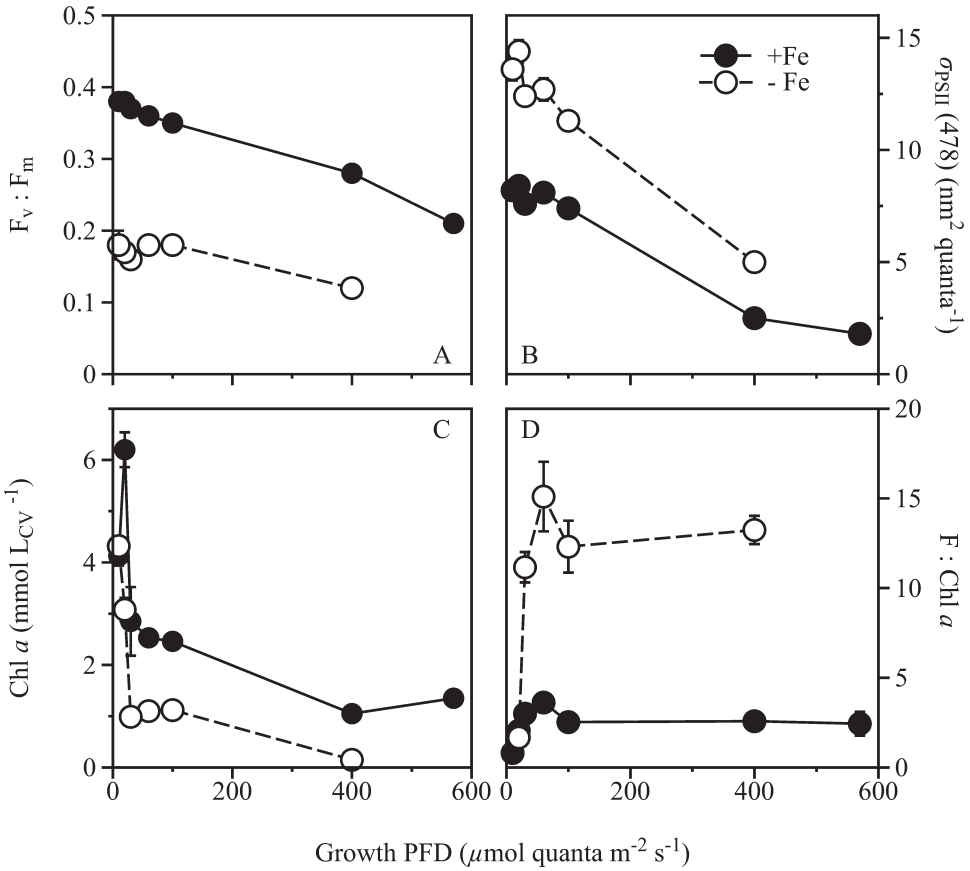

Fig. 6. Photosynthetic characteristics of iron-replete and iron-limited cultures of *P. antarctica* (clone AA1) grown over a range of photon flux densities. (A) The maximum photochemical efficiency of PSII ($F_v : F_m$) measured with a single turnover (ST, FRR) saturation protocol. (B) Functional absorption cross section of PSII (σ_{PSII} (478)). (C) Cell volume–normalized Chl *a* concentrations. (D) In vivo Chl *a* fluorescence normalized to cellular Chl *a* concentration. Error bars represent standard error and are smaller than the symbol when not visible (n = 3–9).

(Sunda and Huntsman 1997; Galbraith et al. 2010), and how to define such co-regulation or co-limitation (Saito et al. 2008). Central to this debate is the concept that light may modulate the cellular iron requirements of phytoplankton, thereby affecting both the onset and degree of iron limitation in natural systems, and consequently the magnitude of carbon fixation. However, the extent to which the trends reported for the interplay of iron and light on temperate phytoplankton species, from both coastal and offshore waters (Sunda and Huntsman 1997), apply to the S. Ocean is not known. To the best of our knowledge, our study is the first systematic examination of the effect of light on the cellular iron requirements of S. Ocean species. Here, we discuss the factors that influence intracellular iron content and Fe : C molar ratios of each phytoplankton species as they encounter changes in iron and light supply. Then, we discuss the physiological evidence for the absence of iron–light antagonism in S. Ocean phytoplankton. We conclude with a short discussion on the regional biogeochemical implications of our findings regarding the influence of iron and light in modifying the iron requirements of S. Ocean phytoplankton.

Defining iron–light co-limitation—In this study, we define iron–light co-limitation following that proposed by Arrigo (2005), as expanded upon by Saito et al. (2008)—"Type III. Biochemically dependent co-limitation." This refers to the limitation of one resource that manifests itself in an inability to acquire another resource. By this definition, although both resources may be limiting, only one is required to elicit a growth response. In the specific case of iron and light, it has been argued that iron limitation results in a decreased capacity to acquire photons from a reduction in the iron-rich photosynthetic units (Sunda and Huntsman 1997). Therefore, by increasing either the supply of photons or iron, this co-limitation is at least partially alleviated, with the greatest relief afforded when both resources are supplied concomitantly. Such a response has been observed in resident phytoplankton of the northeast subarctic Pacific and taken as evidence for an antagonistic low iron–low light co-limitation (Maldonado et al. 1999). We also observed such a response, to varying degrees, in all of the species we examined (Fig. 2). However, as we will argue below, although this physiological response to increases in iron and/or light is difficult to distinguish from the

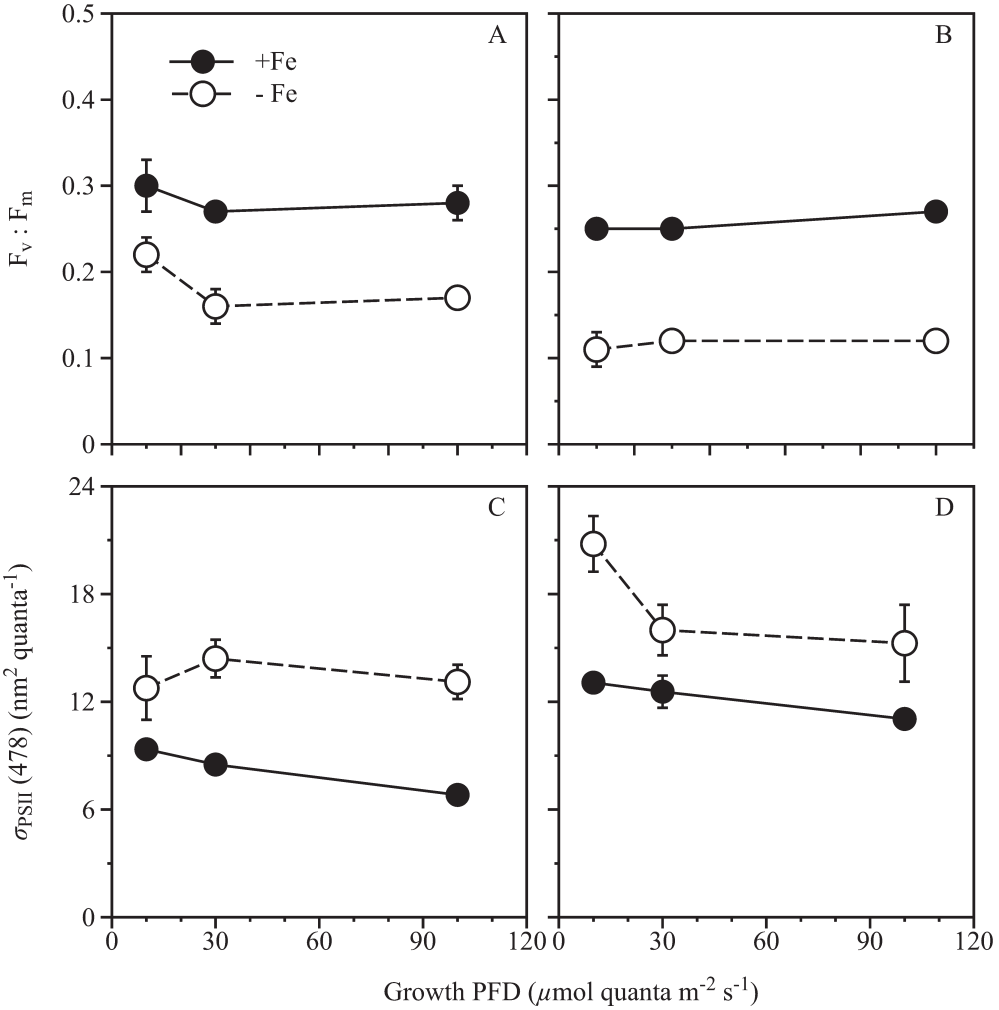

Fig. 7. Photosynthetic characteristics of iron-replete and iron-limited cultures of the S. Ocean diatoms (A, C) *E. antarctica* and (B, D) *P. inermis*. (A, B) $F_v : F_m$ measured with a single turnover (ST, FRR) saturation protocol. (C, D) Functional absorption cross section of PSII (σ_{PSII} (478)). Error bars represent standard error and are smaller than the symbol when not visible.

traditional view of antagonistic iron–light co-limitation, the underlying mechanism is fundamentally different in S. Ocean isolates. Additionally, less attention has been paid to the converse co-limitation dependence, where light influences the acquisition of iron. Our data suggest that light may affect iron uptake not only through changes in iron chemistry, but also at the physiological level.

Iron uptake and cellular iron content—Previous laboratory studies of temperate phytoplankton have revealed that decreasing light intensity substantially increases the cellular Fe : C ratio needed to support a given growth rate (Sunda and Huntsman 1997, 2011). This effect of decreasing light intensity was predicted theoretically (Raven 1990) and verified empirically with both laboratory cultures of temperate diatom species (Strzepek and Harrison 2004), and resident communities from high-latitude HNLC (Maldonado et al. 1999) and low-latitude subsurface (Hopkinson and Barbeau 2008) waters. In contrast to these previous studies, in our S. Ocean isolates, decreasing the light intensity had a negligible effect on the cellular Fe : C ratio required to support a given growth rate, whether growth was expressed in absolute or relative terms (Fig. 5A,C). In order to understand the behavior of the S. Ocean species, we must first reexamine the theoretical considerations for why cellular iron requirements may change with variations in light intensity.

Phytoplankton growing at light intensities sub-saturating for growth are limited due to light absorption by chlorophyll, which in turn decreases rates of photosynthesis and growth. Cells can acclimate to low light conditions in one of two ways, which are not mutually exclusive (Fig. 1). Photoacclimation to low light by increasing the number of photosynthetic units (PSUs) requires a substantial increase in intracellular iron, as each unit is comprised of iron-rich proteins that catalyze photosynthetic electron transport

(Sunda and Huntsman 1997). For example, quantitative analysis of these iron-rich proteins conducted by Strzepek and Harrison (2004) provided not only a biochemical explanation for the lower cellular iron requirements of *T. oceanica* compared to *T. weissflogii*, but also revealed that photosynthetic iron requirements increase in both species under light limitation. In contrast, photoacclimation by increasing PSU size (i.e., the ratio of Chl *a* and other light-harvesting pigments to photosynthetic reaction centers) can also increase light absorption (Falkowski and La Roche 1991), but does not require an increase in intracellular iron. However, Raven (1990) suggested that increasing PSU size decreases the efficiency of excitation energy transfer from light-harvesting pigments to photosynthetic reaction centers, and that this inefficiency ultimately limits the maximum size of PSUs.

Sunda and Huntsman (1997) observed that although cells need higher Fe : C ratios for growth under low light, low-light-acclimated cells did not require higher external iron concentrations to achieve maximum growth rate. The authors proposed a "biodilution" mechanism to explain this counterintuitive result, whereby as light is decreased, μ decreases because of light limitation but the iron uptake rate remains constant or decreases less than that of the specific growth rate. Indeed, for the temperate diatom and dinoflagellate species they examined, the relationships between iron uptake rates and [Fe′] were independent of light intensity. The decrease in growth rate with light limitation caused intracellular iron concentrations to increase because of the inverse relationship between intracellular iron and μ at constant steady-state iron uptake rate, V_{ss}:

$$\text{Intracellular Fe} = V_{ss}/\mu \quad (5)$$

This inherent growth-related negative feedback was argued to help cells to photoacclimate, as they can then use the additional cellular iron to synthesize more PSUs.

We observed that intracellular iron concentrations increased, decreased, or remained constant with decreasing light intensity, depending on the phytoplankton species (i.e., temperate vs. polar) and whether the cultures were iron-replete or iron-limited. Moreover, in some cases we observed light- and iron-dependent changes in cell volumes and cellular carbon concentrations that either amplified or attenuated the variations in intracellular iron content with changes in light intensity. Thus, the interpretation of our results depends on whether iron content is normalized per cell, per unit cell volume, or relative to cellular carbon.

In the case of iron-replete temperate diatom cultures growing in Fe-EDTA media, we observed that in both species changes in μ, V_{ss}, and cellular carbon concentration were proportional. Although reduction in cell size was not a universal response to iron and/or light limitation (Table 1), a reduction in cell volume with decreasing irradiance was the principal cause for the increase in intracellular iron concentrations in iron-replete cultures of *T. weissflogii*. Furthermore, iron uptake and growth rates were closely coupled in iron-limited cultures of *T. weissflogii*. Here, the increase in Fe : C ratios with decreasing light was due to decreases in cellular carbon relative to iron. However, the data for iron-limited cultures of *T. oceanica* supported a "biodilution" mechanism. Changes in the Fe : C ratio of iron-limited *T. oceanica* were driven principally by increasing intracellular iron concentrations with decreasing light, as steady-state iron uptake rates differed little but specific growth rates declined 2.3-fold with decreasing irradiance. Thus, our findings on these temperate diatom species both partially support those of Sunda and Huntsman (1997) but also suggest that these iron–light interactions are more complex than previously reported, with modifications in cell size affecting iron and carbon concentrations and independent changes in cellular iron and carbon concentrations causing shifts in elemental stoichiometry.

Since phytoplankton have considerable variation in their maximum and minimum cellular iron content (Marchetti et al. 2006), and the ability to store iron in excess of cellular iron requirements when iron supply exceeds demand, we cannot reliably infer how cellular iron requirements change with irradiance in iron-replete cultures. However, our results do provide some insights as to how growth irradiance affects the balance between growth and iron acquisition rates. We observed that intracellular iron concentrations increased 7.9-fold in *E. antarctica* and 5.3-fold in *P. inermis* with increasing light in iron-replete cultures grown in Fe-EDTA medium (Table 1; Fig. 4). Intracellular iron concentrations of iron-replete *P. antarctica* cultures also increased with increasing light but plateaued at [Fe′] approaching the threshold for precipitation of iron hydroxides (Sunda and Huntsman 1995). This effect is likely due in part to the increase in the photo-redox cycling of Fe-EDTA chelates and hence [Fe′] at higher irradiances. However, the changes in iron uptake with light were much greater than changes in [Fe′] (2.6-fold), suggesting that light may also influence rates of iron acquisition at the physiological level.

Although most experiments of iron uptake and iron reductase activity in marine phytoplankton have been conducted in the dark to avoid photochemical reactions (Maldonado and Price 2001), recent data show that iron uptake from non-photolabile Fe-DFB complexes during short-term experiments (8–15 h) by *P. antarctica* (that possesses an iron chelate reductase pathway) was 2-fold higher in the light compared to dark (Strzepek et al. 2011). As the Fe-DFB complex is not photo-reactive, these results suggested that the bioreductive iron acquisition pathway might be enhanced in the light, presumably fueled by products derived from photosynthesis. Temperate diatoms grown in Fe-EDTA media are also subject to light-mediated changes in [Fe′]. Because cellular iron concentrations tended to increase with decreasing light (and hence decreasing [Fe′]) in iron-limited cultures, it would appear that for these temperate diatoms changes in the balance between iron uptake and growth have a greater influence on setting cellular iron concentrations than alteration of iron chemistry.

In iron-limited S. Ocean diatom cultures, we observed that steady-state iron uptake rates decreased less than specific growth rates with declining light. Consequently, intracellular iron concentrations were 1.9- and 1.5-fold

higher at 10 μmol quanta m^{-2} s^{-1} compared to 100 μmol quanta m^{-2} s^{-1} in *E. antarctica* and *P. inermis*, respectively. However, cellular carbon concentrations increased in concert with intracellular iron, resulting in relatively constant cellular Fe : C ratios. Thus, our findings suggest that cellular iron demand does not change appreciably as cells acclimate to low light and provide only limited support of the "biodilution" hypothesis for S. Ocean diatoms.

Modes of photoacclimation: PSU number vs. PSU size—In *P. antarctica*, for which we have a comprehensive data set of both intracellular iron and cellular Chl *a* concentrations, acclimation to lower light intensities (from 400 to 10 μmol quanta m^{-2} s^{-1}) increased the Chl *a* : Fe ratios in iron-limited and iron-replete cells by 34- and 9-fold, respectively, while changes in the Fe : C ratio needed to support a given growth rate were negligible (Fig. 5). Here, photoacclimation appears to involve principally an increase in the size of PSUs and not the number. This conclusion is supported by the 3.2- and 2.7-fold increases in σ_{PSII} in iron-replete and iron-limited cells with decreasing irradiance (Fig. 6). So far as we are aware, the phenotypic plasticity in σ_{PSII} that we observed for *P. antarctica* is unprecedented, and compares with the at most 1.5-fold change observed in other phytoplankton species over a comparable irradiance range (Kolber et al. 1988; Suggett et al. 2004).

We also observed that σ_{PSII} was very large in the S. Ocean diatoms (12.8 $\pm$ 3.7 nm^2 $quanta^{-1}$; mean $\pm$ SD of all treatments, both species) compared to published values for coastal diatom isolates ($\sim$ 2–5 nm^2 $quanta^{-1}$; Suggett et al. 2009)—we are not aware of any previously published σ_{PSII} values for S. Ocean laboratory cultures. Indeed, the large σ_{PSII} and low maximum $F_v : F_m$ of these S. Ocean diatoms are at the extreme upper (and lower) limits for eukaryotic algae (Suggett et al. 2009). Suggett et al. (2009) observed a negative correlation between σ_{PSII} and $F_v : F_m$, and taxon-related shifts in these variables that broadly corresponded with cell size, such that large diatoms had high $F_v : F_m$ and low σ_{PSII}, and small nanoflagellates (pelagophytes and prasinophytes) had low $F_v : F_m$ and high σ_{PSII}. From a photo-physiological perspective, S. Ocean diatoms have functional traits more akin to these small cells that tend to dominate nutrient-poor oceanic waters (Suggett et al. 2009). Our results are thus consistent with the hypothesis that resource limitation acts as a selective pressure to maximize light harvesting while reducing the cellular resources required for the production of reaction centers (Strzepek and Harrison 2004). However, as we discuss below, our results also suggest that S. Ocean diatoms have somehow adopted this strategy despite their large size.

While our σ_{PSII} values are large in relation to those for temperate coastal diatoms, they are consistent with estimates obtained for resident S. Ocean phytoplankton communities ($\sim$ 5 to 10 nm^2 $quanta^{-1}$; Sosik and Olson 2002; Moore et al. 2007). Large σ_{PSII}, coupled with lower intracellular iron concentrations (assuming that the majority of intracellular iron is within the photosynthetic electron transport chain), strongly suggest that S. Ocean diatoms have even larger light-harvesting antennae (larger PSU sizes) transferring excitation energy to fewer iron-rich photosynthetic reaction centers (lower PSU numbers) than *P. antarctica*. Furthermore, we propose that S. Ocean species acclimate to irradiance primarily through changes in PSU size rather than number. Such speculation supports the predictions of Raven (1990) that led to the antagonistic iron–light co-limitation hypothesis. However, our results also suggest that even with the reduced efficiency inherent in large PSU size, excitation energy transfer from the antennae to the reaction centers is sufficient for the growth of S. Ocean species under low-temperature conditions.

There are both benefits and drawbacks to large PSU sizes as opposed to PSU numbers, and S. Ocean diatoms appear to have overcome some if not all of these issues. For example, changes in PSU size will decrease the resource (i.e., iron) costs of photoacclimation to low light, but at the expense of potentially decreasing light absorption due to self-shading, particularly in large cells that are more subject to reductions in the efficiency of light absorption per unit pigment (i.e., the "package effect"). However, we observed that while the physical size of S. Ocean diatoms (i.e., based on the frustule) is large, they contain significantly less cellular material per unit cell volume than smaller cells such as *P. antarctica*, *T. oceanica*, and *T. weissflogii*. A comparison of the cellular carbon content normalized to cell volume of the largest S. Ocean diatom we studied, *P. inermis*, reveals that it is 3.3–7.8-fold lower in iron-replete cells and 3.3–18-fold lower in iron-limited cells than in *P. antarctica* (Table 1). The decreased cytoplasm to cell volume ratio of large cells is well documented (Behrenfeld et al. 2008). In addition to decreasing self-shading (Finkel and Irwin 2000), and thereby enhancing the efficiency of light absorption, the maintenance of a large frustule size (but low cytoplasm to cell volume ratio) potentially increases the capacity for luxury storage of nutrients such as iron in vacuoles while reducing mortality through grazing (Smetacek et al. 2004).

One disadvantage of this photoacclimatory strategy is the reduced efficiency of excitation energy transfer from the light-harvesting antennae to the reaction centers, which may account for the inherently lower maximum $F_v : F_m$ values of S. Ocean species under optimal growth conditions. Indeed, a decrease in photochemical efficiency ($F_v : F_m$) with a larger light-harvesting antennae size (larger σ_{PSII}) is expected in energetic terms because higher pigment content extends the lifetime of excitation energy within the antenna. This raises the probability that absorbed light energy will be dissipated as heat rather than contributing to photochemistry (Suggett et al. 2009). Such a reduction in photosynthetic efficiency may not be so disadvantageous in S. Ocean waters, since low temperature constrains maximum photosynthetic and growth rates (*see* discussion in Galbraith et al. 2010). However, the combination of large PSU size and temperature-constrained photosynthetic processes "downstream" from light absorption would likely be disadvantageous at high light, particularly if these reactions were further constrained by iron limitation.

Our results for *P. antarctica* are in excellent agreement with those of Arrigo et al. (2010), who observed that the

growth of iron-replete cultures of *P. antarctica* were inhibited under continuous growth irradiances exceeding 65 μmol quanta m^{-2} s^{-1}. In our experiments, iron limitation exacerbated the effect of high irradiance. For example, iron-limited cultures were unable to grow at the highest irradiance tested (570 μmol quanta m^{-2} s^{-1}). It should be noted, however, that several aspects of our experimental design likely accentuated the deleterious combination of high irradiance and low iron supply. First, our experiments were performed using continuous irradiance. *P. antarctica* has been reported to have a photoprotective strategy that relies heavily upon protein synthesis, presumably for the repair of damaged D1 protein within the PSII reaction center (Kropuenske et al. 2009). Therefore, by growing cultures under continuous light, we may have negatively altered the balance between PSII damage and repair. Second, we used the non-photolabile Fe-DFB complex as an iron source for iron-limited cultures. Increases in iron availability due to enhanced photo-redox iron cycling at higher light may counter the negative effects of supraoptimal irradiances somewhat in natural seawater (Fan 2008). Despite these methodological issues, our results add to the growing evidence that natural populations of S. Ocean phytoplankton, growing under a diel cycle, and likely in the presence of photo-labile iron–ligand complexes (Fan 2008), are nevertheless sensitive to high light, with the combination of low iron and high light being particularly deleterious (Moore et al. 2007; Hoffman et al. 2008; Alderkamp et al. 2010, 2012). Thus, there is circumstantial evidence to support our proposed strategy of an increase in PSU size as opposed to PSU number.

Physiological evidence against iron–light antagonism—Under the current paradigm, we would expect that if iron uptake rates did not exceed growth rates at low light, and hence the cells were unable to fulfill their additional iron demands, they would be more subject to iron limitation at low light. However, we observed the opposite. Both of the iron-limited S. Ocean diatoms that we examined had higher $\mu_{-Fe}:\mu_{+Fe}$ and comparable $F_v:F_m$ at low light vs. high light, while maintaining relatively constant intracellular iron concentrations and cellular Fe : C ratios. Moreover, the particularly detailed data set available for *P. antarctica* (clone AA1) provides strong support for this conclusion. As in the S. Ocean diatoms, $\mu_{-Fe}:\mu_{+Fe}$ and $F_v:F_m$ increased with decreasing light. Additionally, iron-limited cells acclimated to low light had comparable cellular Chl *a* concentrations to iron-replete cells, suggesting that iron limitation impaired neither Chl *a* synthesis nor low-light photoacclimation. Finally, F : Chl *a* was comparably low in iron-replete and iron-limited cultures grown at low light, suggesting that the rise in F : Chl *a* ratios observed in iron-limited cultures as light increased was due principally to the uncoupling of PSII antennae from photo-damaged PSII reaction centers (Vassiliev et al. 1995). In combination, the growth rate, elemental, and photo-physiological data provide compelling evidence that in our experiments S. Ocean phytoplankton were not co-limited antagonistically by low iron and light availability.

In order to further support our assertion of the absence of antagonistic low iron–low light co-limitation for our S. Ocean isolates, we need to reconcile our observation of reduced IUEs at low light. We observed an ~ 2-fold reduction in IUEs in both S. Ocean and temperate isolates with decreasing light. This reduction is essentially as predicted by Raven (1990): that cells at low light "require" higher iron per carbon per unit time than cells at high light. A fundamental problem with this argument, however, is that by definition light-limited cells are limited by light absorption and not photosynthetic electron transport. IUEs will inevitably decrease at lower irradiances as growth slows, unless there are proportional reductions in cellular Fe : C. Presumably, there are genotypic constraints on the minimum number of reaction centers. In the most extreme case of light limitation (i.e., darkness), S. Ocean diatoms, including *P. inermis*, appear to retain a functional photosynthetic electron transport chain (Peters and Thomas 1996). These diatoms rapidly resume photosynthesis (within 24 h) after prolonged periods of darkness (up to 10 months), suggesting that the photosynthetic electron transport chain is maintained in the absence of light. Such an adaptation is likely important for phytoplankton that overwinter in S. Ocean waters and rapidly resume growth in response to more favorable irradiance conditions in the spring. Future research focused on quantifying photosystem stoichiometry and abundance, and maximum achievable electron transfer rates through these complexes, would help to refine estimates of cellular iron demand, and how this demand is altered by changes of both iron and light supply.

Redefining iron–light co-limitation—The field-based observation that the greatest physiological response is observed when iron and light are provided together (Maldonado et al. 1999; Moore et al. 2007) has been taken as evidence for an antagonist iron–light relationship: i.e., more iron is needed for photosynthesis at low light. However, our results suggest that the cellular iron requirements of S. Ocean phytoplankton are no higher at low light than at high light. We attribute this difference to contrasting photoacclimatory strategies (Fig. 1). Nevertheless, the growth of S. Ocean phytoplankton is stimulated when iron and light are supplied together. We therefore propose an alternative explanation for the synergistic effects of elevated light and iron supply. If iron but not light supply is increased, cell growth is still limited by light absorption. Conversely, if light, but not iron supply is increased, cells are unable to use the light they absorb due to a lack of iron (light absorption is no longer the rate-limiting step; the iron-rich electron transfer process is constrained). This imbalance between light absorption and photochemical conversion would tend to exacerbate photoinhibition. Cells can only use higher light when provided enough iron to effectively catalyze photosynthetic electron transport. The phenomenon would be difficult to distinguish from the alleviation of low-light, low-iron biochemical co-limitation (Type III), but the mechanism is fundamentally different (*see* fig. 2 of Saito et al. 2008). If this proposal is correct, it would suggest that antagonistic iron–light co-limitation is more appropriately defined as "Type 1: Independent co-limitation" as defined by Saito et

al. (2008) and used by Moore et al. (2004) to model iron–light interactions on phytoplankton physiology. Furthermore, our results highlight the difficulty of characterizing iron–light co-limitation in the field, and the potential for misattribution of the causal factors responsible for the observed responses to bioassay experiments.

Implications of iron–light interaction for S. Ocean biogeochemistry—The S. Ocean plays a disproportionate role in carbon biogeochemistry and global climate, and thus has been the focus of regional biogeochemical modeling studies (Tagliabue and Arrigo 2005). Our main conclusion, the absence of an antagonistic iron–light co-limitation in the S. Ocean phytoplankton species we studied, suggests that biogeochemical models that have used this relationship to parameterize their models may have both overestimated phytoplankton iron requirements and also the areal extent of iron limitation in S. Ocean waters. Our findings may provide a clearer understanding of how low light and iron supply influences S. Ocean phytoplankton and enable a more accurate parameterization of regional biogeochemical models. The absence of biochemical iron–light co-limitation for S. Ocean phytoplankton will have additional ramifications. For example, it may help to simplify our understanding of the interplay of environmental controls and how they vary with both season and region in the S. Ocean (Boyd 2002; Boyd et al. 2010). The lack of this antagonistic co-limitation in S. Ocean waters but its presence outside of S. Ocean waters also means that iron and light limitation will have to be represented by two distinct parameterizations in global ocean biogeochemical models.

Acknowledgments

We thank Sylvia Sander and Fien Tian for electrochemical Fe analyses. We thank Kelly Strzepek, Evelyn Armstrong, and the anonymous reviewers for insightful comments that improved the manuscript. Funding for this work was provided by grants from the Marsden Fund of New Zealand and the Ministry of Science and Innovation (MSI) New Zealand.

References

Alderkamp, A., H. J. W. de Baar, R. J. W. Visser, and K. R. Arrigo. 2010. Can photoinhibition control phytoplankton abundance in deeply mixed water columns of the Southern Ocean? Limnol. Oceanogr. **55:** 1248–1264, doi:10.4319/lo.2010.55.3.1248

———, G. Kulk, A. G. J. Buma, R. J. W. Visser, G. L. Van Dijken, M. M. Mills, and K. R. Arrigo. 2012. The effect of iron limitation on the photophysiology of *Phaeocystis antarctica* (Prymnesiophyceae) and *Fragilariopsis cylindrus* (Bacillariophyceae) under dynamic irradiance. J. Phycol. **48:** 45–59, doi:10.1111/j.1529-8817.2011.01098.x

Arrigo, K. R. 2005. Marine microorganisms and global nutrient cycles. Nature **437:** 349–355, doi:10.1038/nature04159

———, M. M. Mills, L. R. Kropuenske, G. L. van Dijken, A. Alderkamp, and D. H. Robinson. 2010. Photophysiology in two major Southern Ocean phytoplankton taxa: Photosynthesis and growth of *Phaeocystis antarctica* and *Fragilariopsis cylindrus* under different irradiance levels. Integr. Comp. Biol. **50:** 950–966, doi:10.1093/icb/icq021

Aumont, O., and L. Bopp. 2006. Globalizing results from ocean in situ iron fertilization studies. Global Biogeochem. Cycles **20:** GB2017, doi:10.1029/2005GB002591

Behrenfeld, M. J., K. H. Halsey, and A. J. Milligan. 2008. Evolved physiological responses of phytoplankton to their integrated growth environment. Phil. Trans. R. Soc. B **363:** 2687–2703, doi:10.1098/rstb.2008.0019

Boyd, P., J. La Roche, M. Gall, R. Frew, and R. M. L. McKay. 1999. Role of iron, light, and silicate in controlling algal biomass in subantarctic waters SE of New Zealand. J. Geophys. Res. **104:** 13395–13408, doi:10.1029/1999JC900009

Boyd, P. W. 2002. Environmental factors controlling phytoplankton processes in the Southern Ocean. J. Phycol. **38:** 844–861, doi:10.1046/j.1529-8817.2002.t01-1-01203.x

———, A. C. Crossley, G. R. Ditullio, F. B. Griffiths, D. A. Hutchins, B. Queguiner, P. N. Sedwick, and T. W. Trull. 2001. Control of phytoplankton growth by iron supply and irradiance in the subantarctic Southern Ocean: Experimental results from the SAZ Project. J. Geophys. Res. **106:** 31573–31583, doi:10.1029/2000JC000348

———, T. Jickells, C. S. Law, S. Blain, E. A. Boyle, K. O. Buesseler, K. H. Coale, J. J. Cullen, H. J. W. de Baar, M. Follows, M. Harvey, C. Lancelot, M. Levasseur, N. P. J. Owens, R. Pollard, R. B. Rivkin, J. Sarmiento, V. Schoemann, V. Smetacek, S. Takeda, A. Tsuda, S. Turner, and A. J. Watson. 2007. Mesoscale iron enrichment experiments 1993–2005: Synthesis and future directions. Science **315:** 612–617, doi:10.1126/science.1131669

———, R. F. Strzepek, F. X. Fu, and D. A. Hutchins. 2010. Environmental control of open ocean phytoplankton groups: Now and in the future. Limnol. Oceanogr. **55:** 1353–1376, doi:10.4319/lo.2010.55.3.1353

Cullen, J. J., and R. F. Davis. 2003. The blank can make a big difference in oceanographic measurements. Limnol. Oceanogr. Bull. **12:** 29–35.

Falkowski, P. G., and J. La Roche. 1991. Acclimation to spectral irradiance in algae. J. Phycol. **27:** 8–14, doi:10.1111/j.0022-3646.1991.00008.x

Fan, S. M. 2008. Photochemical and biochemical controls on reactive oxygen and iron speciation in the pelagic surface ocean. Mar. Chem. **109:** 152–164, doi:10.1016/j.marchem.2008.01.005

Finkel, Z. V., and A. J. Irwin. 2000. Modeling size-dependent photosynthesis: Light absorption and the allometric rule. J. Theor. Biol. **204:** 361–369, doi:10.1006/jtbi.2000.2020

———, A. Quigg, J. A. Raven, J. R. Reinfelder, O. E. Schofield, and P. G. Falkowski. 2006. Irradiance and the elemental stoichiometry of marine phytoplankton. Limnol. Oceanogr. **51:** 2690–2701, doi:10.4319/lo.2006.51.6.2690

Galbraith, E. D., A. Gnanadesikan, J. P. Dunne, and M. R. Hiscock. 2010. Regional impacts of iron–light colimitation in a global biogeochemical model. Biogeosciences **7:** 1043–1064, doi:10.5194/bg-7-1043-2010

Hiscock, M. R., V. P. Lance, A. Apprill, R. R. Bidigare, Z. I. Johnson, B. G. Mitchell, W. O. Smith, and R. T. Barber. 2008. Photosynthetic maximum quantum yield increases are an essential component of the Southern Ocean phytoplankton response to iron. Proc. Natl. Acad. Sci. USA **105:** 4775–4780, doi:10.1073/pnas.0705006105

Hoffman, L. J., I. Peeken, and K. Lochte. 2008. Iron, silicate, and light co-limitation of three Southern Ocean diatom species. Polar Biol. **31:** 1067–1080, doi:10.1007/s00300-008-0448-6

Hopkinson, B. M., and K. A. Barbeau. 2008. Interactive influences of iron and light limitation on phytoplankton at subsurface chlorophyll maxima in the eastern North Pacific. Limnol. Oceanogr. **53:** 1303–1318, doi:10.4319/lo.2008.53.4.1303

———, B. G. Mitchell, R. A. Reynolds, H. Wang, K. E. Selph, C. I. Measures, C. D. Hewes, O. Holm-Hansen, and K. A. Barbeau. 2007. Iron limitation across chlorophyll gradients in the southern Drake Passage: Phytoplankton responses to iron addition and photosynthetic indicators of iron stress. Limnol. Oceanogr. **52:** 2540–2554, doi:10.4319/lo.2007.52.6.2540

Kolber, Z., J. Zehr, and P. Falkowski. 1988. Effects of growth irradiance and nitrogen limitation on photosynthetic energy conversion in photosystem II. Plant Physiol. **88:** 923–929, doi:10.1104/pp.88.3.923

Kolber, Z. S., O. Prášil, and P. G. Falkowski. 1998. Measurements of variable chlorophyll fluorescence using fast repetition rate techniques: Defining methodology and experimental protocols. Biochim. Biophys. Acta **1367:** 88–106, doi:10.1016/S0005-2728(98)00135-2

Kropuenske, L. R., M. M. Mills, G. L. van Dijken, S. Bailey, D. H. Robinson, N. A. Welschmeyer, and K. R. Arrigo. 2009. Photophysiology in two major Southern Ocean phytoplankton taxa: Photoprotection in *Phaeocystis antarctica* and *Fragilariopsis cylindrus*. Limnol. Oceanogr. **54:** 1176–1196, doi:10.4319/lo.2009.54.4.1176

Laney, S. R., and R. M. Letelier. 2008. Artifacts in measurements of chlorophyll fluorescence transients, with specific application to fast repetition rate fluorometry. Limnol. Oceanogr.: Methods **6:** 40–50, doi:10.4319/lom.2008.6.40

Macintyre, H. L., T. M. Kana, T. Anning, and R. J. Geider. 2002. Photoacclimation of photosynthesis irradiance response curves and photosynthetic pigments in microalgae and cyanobacteria. J. Phycol. **38:** 17–38, doi:10.1046/j.1529-8817.2002.00094.x

Maldonado, M. T., P. W. Boyd, P. J. Harrison, and N. M. Price. 1999. Co-limitation of phytoplankton growth by light and Fe during winter in the NE subarctic Pacific Ocean. Deep-Sea Res. II **46:** 2475–2485, doi:10.1016/S0967-0645(99)00072-7

———, and N. M. Price. 2001. Reduction and transport of organically bound iron by *Thalassiosira oceanica* (Bacillariophyceae). J. Phycol. **37:** 298–309, doi:10.1046/j.1529-8817.2001.037002298.x

———, R. F. Strzepek, S. Sander, and P. W. Boyd. 2005. Acquisition of iron bound to strong organic complexes, with different Fe-binding groups and photochemical reactivities, by plankton communities in Fe-limited subantarctic waters. Glob. Biogeochem. Cycles **19:** GB4S23, doi:10.1029/2005GB002481

Marchetti, A., M. T. Maldonado, E. S. Lane, and P. J. Harrison. 2006. Iron requirements of the pennate diatom *Pseudo-nitzschia*: Comparison of oceanic (high-nitrate, low-chlorophyll waters) and coastal species. Limnol. Oceanogr. **51:** 2092–2101, doi:10.4319/lo.2006.51.5.2092

Mitchell, B. G., E. A. Brody, O. Holm-Hansen, C. McClain, and J. Bishop. 1991. Light limitation of phytoplankton biomass and macronutrient utilization in the Southern Ocean. Limnol. Oceanogr. **36:** 1662–1677, doi:10.4319/lo.1991.36.8.1662

Moore, C. M., S. Seeyave, A. E. Hickman, J. T. Allen, M. I. Lucas, H. Planquette, R. T. Pollard, and A. J. Poulton. 2007. Iron–light interactions during the CROZet natural iron bloom and Export experiment (CROZEX) I: Phytoplankton growth and photophysiology. Deep-Sea Res. II **54:** 2045–2065, doi:10.1016/j.dsr2.2007.06.011

Moore, J. K., S. C. Doney, and K. Lindsay. 2004. Upper ocean ecosystem dynamics and iron cycling in a global 3-D model. Global Biogeochem. Cycles **18:** GB4028, doi:10.1029/2004GB002220

Mongin, M., D. M. Nelson, P. Pondaven, and P. Tréguer. 2007. Potential phytoplankton responses to iron and stratification changes in the Southern Ocean based on a flexible-composition phytoplankton model. Global Biogeochem. Cycles **21:** GB4020, doi:10.1029/2007GB002972

Nelson, D. M., and W. O. Smith. 1991. Sverdrup revisited: Critical depths, maximum chlorophyll levels, and the control of Southern Ocean productivity by the irradiance-mixing regime. Limnol. Oceanogr. **36:** 1650–1661, doi:10.4319/lo.1991.36.8.1650

Peters, E., and D. N. Thomas. 1996. Prolonged darkness and diatom mortality I: Marine Antarctic species. J. Exp. Mar. Biol. Ecol. **207:** 25–41, doi:10.1016/S0022-0981(96)02520-8

Raven, J. A. 1990. Predictions of Mn and Fe use efficiencies of phototrophic growth as a function of light availability for growth and of C assimilation pathway. New Phytol. **116:** 1–18, doi:10.1111/j.1469-8137.1990.tb00505.x

Saito, M. A., T. J. Goepfert, and J. T. Ritt. 2008. Some thoughts on the concept of colimitation: Three definitions and the importance of bioavailability. Limnol. Oceanogr. **53:** 276–290, doi:10.4319/lo.2008.53.1.0276

Sarmiento, J. L., T. M. C. Hughes, R. J. Stouffer, and S. Manabe. 1998. Simulated response of the ocean carbon cycle to anthropogenic climate warming. Nature **393:** 245–249, doi:10.1038/30455

———, R. Slater, R. Barber, L. Bopp, S. C. Doney, A. C. Hirst, J. Kleypas, R. Matear, U. Mikolajewicz, P. Monfray, V. Soldatov, S. A. Spall, and R. Stouffer. 2004. Response of ocean ecosystems to climate warming. Global Biogeochem. Cycles **18:** GB3003, doi:10.1029/2003GB002134

———, R. D. Slater, J. Dunne, A. Gnanadesikan, and M. R. Hiscock. 2010. Efficiency of small scale carbon mitigation by patch iron fertilization. Biogeosciences **7:** 3593–3624, doi:10.5194/bg-7-3593-2010

Smetacek, V., P. Assmy, and J. Henjes. 2004. The role of grazing in structuring Southern Ocean pelagic ecosystems and biogeochemical cycles. Antarct. Sci. **16:** 541–558, doi:10.1017/S0954102004002317

Sosik, H., and R. J. Olson. 2002. Phytoplankton and iron limitation of photosynthetic efficiency in the Southern Ocean during late summer. Deep-Sea Res. I **49:** 1195–1216, doi:10.1016/S0967-0637(02)00015-8

Strzepek, R. F., and P. J. Harrison. 2004. Photosynthetic architecture differs in coastal and oceanic diatoms. Nature **431:** 689–692, doi:10.1038/nature02954

———, M. T. Maldonado, K. A. Hunter, R. D. Frew, and P. W. Boyd. 2011. Adaptive strategies by Southern Ocean phytoplankton to lessen iron limitation: Uptake of organically complexed iron and reduced cellular iron requirements. Limnol. Oceanogr. **56:** 1983–2002, doi:10.4319/lo.2011.56.6.1983

———, and N. M. Price. 2000. Influence of irradiance and temperature on the iron content of the marine diatom *Thalassiosira weissflogii* (Bacillariophyceae). Mar. Ecol. Prog. Ser. **206:** 107–117, doi:10.3354/meps206107

Suggett, D. J., E. Le Floc'H, G. N. Harris, N. Leonardos, and R. J. Geider. 2007. Different strategies of photoacclimation by two strains of *Emiliania huxleyi* (Haptophyte). J. Phycol. **43:** 1209–1222, doi:10.1111/j.1529-8817.2007.00406.x

———, H. L. Macintyre, and R. J. Geider. 2004. Evaluation of biophysical and optical determinations of light absorption by photosystem II in phytoplankton. Limnol. Oceanogr.: Methods **2:** 316–332, doi:10.4319/lom.2004.2.316

———, C. M. Moore, A. E. Hickman, and R. J. Geider. 2009. Interpretation of fast repetition rate (FRR) fluorescence: Signatures of phytoplankton community structure versus physiological state. Mar. Ecol. Prog. Ser. **376:** 1–19, doi:10.3354/meps07830

Sunda, W. G., and S. A. Huntsman. 1995. Iron uptake and growth limitation in oceanic and coastal phytoplankton. Mar. Chem. **50:** 189–206, doi:10.1016/0304-4203(95)00035-P

———, and ———. 1997. Interrelated influence of iron, light and cell size on marine phytoplankton growth. Nature **390:** 389–392, doi:10.1038/37093

———, and ———. 2003. Effect of pH, light, and temperature on Fe-EDTA chelation and Fe hydrolysis in seawater. Mar. Chem. **84:** 35–47, doi:10.1016/S0304-4203(03)00101-4

———, and ———. 2011. Interactive effects of light and temperature on iron limitation in a marine diatom: Implications for marine productivity and carbon cycling. Limnol. Oceanogr. **56:** 1475–1488, doi:10.4319/lo.2011.56.4.1475

Tagliabue, A., and K. R. Arrigo. 2005. Iron in the Ross Sea: 1. Impact on CO_2 fluxes via variation in phytoplankton functional group and non-Redfield stoichiometry. J. Geophy. Res. **110:** C03009, doi:10.1029/2004JC002531

Timmermans, K. R., M. S. Davey, B. van der Wagt, J. Snoek, R. J. Geider, M. J. W. Veldhuis, L. J. A. Gerringa, and H. J. W. de Baar. 2001. Co-limitation by iron and light of *Chaetoceros brevis*, *C. dichaeta* and *C. calcitrans* (Bacillariophyceae). Mar. Ecol. Prog. Ser. **217:** 287–297, doi:10.3354/meps217287

Vassiliev, I. R., Z. Kolber, K. D. Wyman, D. Mauzerall, V. K. Shukla, and P. G. Falkowski. 1995. Effects of iron limitation on photosystem-II composition and light utilization in *Dunaliella tertiolecta*. Plant Physiol. **109:** 963–972.

Associate editor: Heidi M. Sosik

Received: 26 September 2011
Amended: 04 May 2012
Accepted: 08 May 2012